Iron Isotope Fractionation during Bio- and Photodegradation of Organoferric Colloids in Boreal Humic Waters

Olga Oleinikova, Franck Poitrasson, Olga Yu. Drozdova, Liudmila Shirokova, Sergey Lapitskiy, Oleg Pokrovsky

Iron isotope fractionation during bio- and photo-degradation of organo-ferric colloids in boreal humic waters

Olga V. OLEINIKOVA[1], Franck POITRASSON[1], Olga Yu. DROZDOVA[2], Liudmila S. SHIROKOVA[1,3], Sergey A. LAPITSKIY[2], and Oleg S. POKROVSKY[1,3,4*]

[1] GET (Geosciences and Environment Toulouse) UMR 5563 CNRS, 14 Avenue Edouard Belin, 31400 Toulouse, France
[2] Geological Faculty of Moscow State University, 1 Leninskie Gory, 119234 Moscow, Russia
[3] N. Laverov Federal Center for Integrated Arctic Research, Russian Academy of Science, 23 Naberezhnaya Sev Dviny, Arkhangelsk, Russia
[4] BIO-GEO-CLIM Laboratory, Tomsk State University, 36 Lenina av., 634050 Tomsk, Russia

[*] Corresponding author. *Email address*: oleg.pokrovsky@get.omp.eu (Oleg S. Pokrovsky).

Key words: Fe, heterotrophic bacteria, photolysis, sunlight, Arctic, organic carbon, complexation, size fractionation, oxidation, precipitation

Submitted to *Environ Sci Technol* after revision, September 2019

Key messages:

Adsorption of heavy Fe isotopes on heterotrophic bacteria cell surface

Assimilation of light Fe isotopes by live *P. aureofaciens* cells

Removal of heavy Fe isotopes from solution during sunlight oxidation of organo-ferric colloids

Generation of isotopically light Fe(II) in $LMW_{< 1\ kDa}$ during photolysis

Bio-and photodegradation of organo-ferric colloids can produce very large, from -2.5 to +3.2‰ $\delta^{57}Fe$ isotopic variations in boreal waters

41 **ABSTRACT**

42 Bio-degradation and photolysis of dissolved organic matter (DOM) in boreal high-latitude waters
43 are the two main factors controlling aquatic fluxes and residence time of carbon but also metal
44 nutrients associated with DOM such as Fe. The DOM is usually present in the form of organic and
45 organo-mineral colloids that also account for the majority of dissolved Fe. Here we use the stable Fe
46 isotope approach to unravel the processes controlling Fe behavior during bio- and photo-degradation
47 of colloids in boreal Fe- and DOM-rich humic waters (a stream and a fen). The adsorption of Fe
48 colloids onto heterotrophic bacteria *P. aureofaciens* produced enrichment in +0.4‰ (δ^{57}Fe) in the
49 heavier isotopes of the cell surface relative to the remaining solution. In contrast, long-term
50 assimilation of Fe by live cells yielded preferential incorporation of lighter isotopes into the cells (-
51 0.7‰ relative to aqueous solution). The sunlight-induced oxidation of Fe(II) in fen water led to
52 removal of heavier Fe isotopes (+1.5 to +2.5‰) from solution, consistent with Fe(III) hydroxide
53 precipitation from Fe(II)-bearing solution. Altogether, bio- and photodegradation of organo-ferric
54 colloids, occurring within a few days of exposure time, can produce several per mil isotopic
55 excursions in shallow lentic and lothic inland waters of high latitude boreal regions. Considerable
56 daily scale variations of Fe isotopic composition should therefore be taken into account during
57 interpretation of riverine flux of Fe isotope to the ocean or tracing weathering processes using Fe
58 isotopes in surface waters at high latitudes.

59

60 **1. Introduction**

61 Despite broad use of Fe isotopes for tracing various large-scale, long-term processes at the
62 Earth's surface[1,2], notably in river[3-8] or lake[9,10] waters, the fractionation of Fe isotopes during short-
63 term processes such as bio- and photo-degradation of organic matter that binds Fe in freshwater
64 remain poorly understood. This is especially true for organic carbon and Fe-rich boreal waters, that,
65 from the one hand, play a primary role in the C cycle, CO_2 emissions and storage[11] and from the

other hand, strongly contribute to Fe and other micro-nutrient export by rivers to the coastal productive zones[13,14].

The majority of dissolved (< 0.22 μm) Fe and other metals in boreal waters are present in the form of organic and organo-mineral colloids (1 nm - 0.22 μm) whose transport and bioavailability differ from inorganic ions or simple organic complexes[15]. Two main processes responsible for fluxes and residence time of organic C and metal colloids in boreal high-latitude aquatic environments are heterotrophic bacterial respiration (degradation of DOM) and photolysis[16]. Colloidal transformation often occurs along the hydrological continuum of interconnected soil waters, mires, streams and large oligotrophic lakes[17]. Under the action of aquatic microorganisms and sunlight irradiation, the organic and organo-ferric colloids are subjected to change of dominant source and molecular weight from allochthonous large-size humic and fulvic molecules to small size autochthonous organic ligands[17]. Further, the DOC can be degraded into CO_2 or taken up by heterotrophic bacterioplankton. This may liberate Fe(III) ions, leading to Fe oxy(hydr)oxide precipitation[18,19]. Finally, photooxidation of DOM may lead to enrichment in low molecular weight organic ligands and their complexes with metals[20].

In contrast to numerous works devoted to microbiological[21] and photochemical[22] mineralization of dissolved organic carbon (DOC), nitrogen and phosphorus, the bacterial and sunlight-induced transformations of Fe-rich colloids in inland waters have been little studied[23,24]. The transformation of colloidal Fe in boreal waters, including bogs, lakes and rivers[25] has been studied under the metabolic action of heterotrophic soil and aquatic bacteria[18,26-27] and sunlight[28]. In these works we demonstrated that the biodegradation of organo-ferric colloids by heterotrophic bacteria consists of *i*) element uptake inside the cells; *ii*) element adsorption at the cell surface, and *iii*) Fe hydroxide precipitation leading to scavenging of associated trace metals. During both biodegradation and photolysis of natural DOM, Fe plays a pivotal role in controlling the fate of trace elements (TE). This control occurs via *i*) formation of insoluble Fe(III) hydroxides that coprecipitate other trace

91 metals[28], and *ii*) generation of low molecular weight (LMW) organic ligands that bind Fe, thus
92 competing with strong organic complexes of other metals[19,20,28].

93 The Fe isotope approach is an efficient tool for deciphering elementary processes involving
94 microbes and aqueous solutions[29-33], DOM - Fe[34] and mineral - Fe[35,36] interaction including
95 colloids[3,6, 37]. The latter study demonstrated an unusual enrichment of heavier Fe isotopes in the
96 LMW (< 1-10 kDa) fraction relative to remaining colloidal fraction (by up to +3 to +4 ‰ in δ^{57}Fe)
97 and suggested that bio- and/or photo-transformation of colloids may be responsible for heavy Fe
98 isotope signatures in LMW fraction of boreal waters. However, the photo-oxidation of organo-ferric
99 colloids removes Fe in the form of Fe(III) hydroxides[19,23,38] which can enrich the remaining solution
100 in lighter Fe isotopes, consistent with numerous laboratory experiments on Fe hydroxide
101 precipitation from Fe(II)-bearing aqueous solution[39]. Whereas for $Fe^{3+}(aq) \rightarrow Fe(III)_{solid}$ (hematite)
102 reaction at equilibrium, a negligible fractionation of -0.15±0.30 ‰ (Δ^{57}Fe) was reported[40], the
103 $Fe^{2+}(aq) \rightarrow Fe(III)_{solid}$ (ferrihydrite) reaction has Δ^{57}Fe of +4.8±0.15 ‰[39]. Other experiments
104 producing goethite reported a fractionation factor of +1.7±0.14‰, corresponding to the $Fe(III)_{solid}$
105 being enriched in heavier isotopes[41]. As for the bacterially-induced colloid transformation, two main
106 processes controlling the isotope fractionation during metal-live cell interaction are 1) fast adsorption
107 of heavier Fe isotope on the cell surfaces[30,31], and 2) long-term assimilation of heavier Fe isotopes as
108 recently shown for phytoplankton[42] and magnetotactic bacteria[33]. Note however that, in contrast to
109 the fairly good knowledge of isotope fractionation of ionic metals and their organic complexes
110 interaction with microbial cells, virtually nothing is known on colloidal metal – cell interaction
111 reactions. The present study is aimed at the quantification of Fe isotope signatures during photo- and
112 bio-degradation of DOM-Fe complexes in high latitude boreal waters. We hypothesized preferential
113 removal of heavier Fe isotopes by live cell adsorption and assimilation and Fe hydroxide
114 precipitation in the course of bio- and photodegradation of organo-ferric colloids. We further tested
115 the possibility of formation of isotopically heavy Fe in $LMW_{< 1\ kDa}$ fraction of river waters, as it was
116 put forward in a previous study[37]. To test these hypotheses, we selected a stream and a fen water, two

dominant types of Fe-rich freshwaters of the subarctic. By choosing two main processes controlling the fate of organo-ferric colloids (bio- and photo-degradation) and two representative examples of boreal Fe- and DOM-rich surface waters, we were capable to reveal the main factors that govern Fe isotope behavior on a short-term (daily) scale in large territory of subarctic landscapes.

2. Materials and methods

The surface waters were collected in the Northern Karelia region (NW Russia). The climate of the region is mild-cold, transitional between oceanic and continental. Average temperature in January is -13 °C, and +15 °C in July; average annual precipitation ranges between 450 and 550 mm y^{-1}. Our study area is in the most elevated part of Karelia, within a landscape of tectonic denudation hills, plateaus and ridges with an average altitude of 300-400 m, with separate insulated massifs. Predominant soils are illuvial-humic and illuvial-ferruginous-humic podzols. Coniferous forest (pine and spruce) with some deciduous trees (birch, aspen and alder) dominates the vegetation of the region. Further landscape setting is described in previous works of our group[17,37]. Within the hydrological continuum created by glacial processes around 8-10 thousand years ago, the water and soluble compounds travel from the ombrotrophic peat mire zone downstream the river towards a large oligotrophic lake. At the lake coast, there are minerotrophic fens located in depressions that receive their water via shallow groundwater and soil flux[43].

A small stream and a coastal fen were collected in July 2015, during summer baseflow period. The Palojoki stream (watershed area = 32 km², bedrock of granites, gneisses, syenites, and syenite-diorites of the early-Proterozoic and late-Archean, covered by glacial Quaternary deposits under podzol soils[43]) was sampled in the middle course of the flow (sample KAR-1[17]). The fen adjacent to the western coast of the Tsipringa Lake had an area of 1.19 km^2 and is underlain by Early-Archean biotite granito-gneisses (sample ZPBL[17]).

The experiments included on-site photodegradation of sterile-filtered (< 0.22 μm) stream and fen water in quartz reactors and laboratory microcosm experiments in the presence of 1 g_{wet}/L of *Pseudomonas aureofaciens*, highly abundant culturable bacteria isolated form podzol soils[44]. The

143 experimental scheme described in previous works from our group[27,28] is shown in **Fig. 1**. The
144 biodegradation experiments with stream and fen waters were performed after 6 months storage of
145 sterile-filtered samples in the refrigerator. Freshly-collected bacteria at the stationary growth stage
146 were rinsed in 0.85% NaCl and allowed to starve in nutrient-free 0.85% NaCl solution during 5 days.
147 The cells were rinsed again 3 times before the experiment, concentrated in a mother suspension and
148 added to sterile, acid-washed polypropylene flasks with stream or fen water (typically 2 mL of
149 bacterial suspension to 200 mL of water) to provide the wet biomass concentration of 1 g_{wet} L^{-1}. Note
150 that the amount of Fe originated from bacteria addition does not exceed 1 μg L^{-1} for this
151 concentration of biomass[27]. The flasks were shaken at 25±0.5°C and aerated via Biosilico®
152 ventilation porous caps during 4 days. Aliquots of homogeneous suspension were sampled after 0, 1,
153 8, 22, 30, 50 and 100 h after the addition of bacteria and filtered through 0.22 μm membrane. All the
154 biodegradation experiments were run in duplicates. The control experiment was sterile filtered (<
155 0.22 μm) biomass-free stream and fen water and it was processed exactly as bacterial samples.
156 For photo-degradation experiments, the stream and fen waters were collected in pre-cleaned
157 polypropylene jars and stored in dark cold place (6±2°C) prior the experiments. The waters were
158 processed on-site, within 2 h after sampling, in the field-constructed clean laboratory[37]. Sterile
159 filtration was performed using single-used Sartorius polystyrene vacuum filtration units (0.22 μm,
160 250 mL volume). Filtered fluids were transferred into 270-mL sterilized quartz flasks, filled with
161 10% air headspace and covered by porous sterile stoppers. The dark control of quartz flasks was
162 identical to the light samples except that the reactors were wrapped in Al foil. Both dark and light
163 reactors were run in duplicates and they were placed on flat surface at the border of the lake
164 (66°17'04"N, 30°52'05"E). The flasks were exposed to direct unshaded sunlight from July 9 to July
165 20 during essentially anticyclonic weather. The daytime duration in this period was between 22 and
166 20.5 hours. The temperature of the experimental reactors followed the diurnal cycle and was equal to
167 18 ± 5°C over 250 h of exposure, which was within the range of actual water temperature in stream
168 and fen during the month of July[17,37]. The quartz reactors were sampled after 0, 100 and 200 h of

169 exposure of the fen water (ZPBL) and after 0, 110 and 250 h of exposure of the stream (KAR-1). For
170 each sampling, the whole reactor was sacrificed. The samples were immediately filtered through 0.22
171 μm Sartorius single-used filter into pre-cleaned polypropylene vials. These waters were then
172 acidified using bi-distilled HNO_3 for trace metals analysis or directly used, without acidification, for
173 DOC, $UV_{254\ nm}$, DIC and anions determinations. The 0.22 μm filtrate from quartz reactors was
174 additionally ultrafiltered through 1 and 10 kDa regenerated cellulose single-use filters with an
175 Amicon 8400 frontal Ultrafiltration unit (continuously stirred 400-ml polycarbonate cell maintained
176 under 1.5–2 atm pressure). Details of ultrafiltration procedure in humic boreal waters of North
177 Karelia and discussion of possible artifacts are presented elsewhere[17,37,43]. In these experiments, we
178 consider the behavior of Fe in <0.22 μm and <10 kDa fractions of the stream water and in <0.22 μm,
179 <10 and <1 kDa fractions of the fen water.

180 Analyses of DOC and Fe concentration in various filtered and ultrafiltered fractions were
181 performed using Shimadzu TOC-VCSN and Agilent ICP MS, following procedures described
182 previously[27,28]. The DOC was measured with an uncertainty of 3% and a detection limit of 0.1 mg L^{-1}.
183 The total dissolved Fe represents the sum of Fe(II) and Fe(III) in the < 0.22 μm fraction. The
184 uncertainty of Fe concentration measurements ranged from 5 to 10% (1SD). The international
185 geostandard SLRS-5 (Riverine Water Reference Material for Trace Metals certified by the National
186 Research Council of Canada) measured each 20 samples was used to check the validity and
187 reproducibility of Fe analysis. Good agreements were found between the replicate measurements of
188 Fe in SLRS-5 and the certified values (relative difference < 20% SD on the repeated measurements).

189 Assessment of Fe(II) and Fe(III) concentrations was performed using the conventional
190 ferrozine method[45]. The efficiency of this method in organic-rich tropical waters was further
191 demonstrated in Rio Negro[46]. Because of possible interferences from DOM in humic boreal waters,
192 the ferrozine method was used employing a standard addition technique. This allowed to achieve a
193 detection limit of 15 μg L^{-1} and an uncertainty from 10-20% at 15 < Fe(II) <100 μg L^{-1} to 5-10% at
194 Fe(II) > 100 μg L^{-1}. Further, we verified the stability of Fe(II) in oxygenated humic waters (pH = 4.6

195 to 6.5; DOC = 20 to 50 mg L^{-1}) using peat and moss leachate (similar to main allochthonous DOM in
196 studied sites[47]). The Fe(II) concentration remained stable within ±10% over 24-180 h of exposure.
197 The Fe(III) and Fe(II) complexation with organic ligands and solution saturation degree with
198 respect to secondary Fe hydroxide in the course of experiment were calculated using Visual
199 MINTEQ[48], in conjunction with a NICA-Donnan humic ion bonding model, as described
200 previously[17]. We considered carboxylic and phenolic complexes of fulvic acids with Fe^{2+} and Fe^{3+}
201 ions, as well as Fe(II) weak (electrostatic) interaction with fulvic acids.
202 For Fe isotope analysis, filtered and acidified water samples were evaporated in the clean
203 laboratory. After acid digestion of the residue using a mixture of HCl and HNO_3, Fe was purified via
204 anion exchange chromatography with HCl using Bio Rad AG1 X4 resin, 200–400 mesh to remove
205 all matrix elements[37]. For this, we used thermoretractable Teflon columns with an internal diameter
206 of 4 mm[8]. The resins were conditioned using 6 M of HCl prior to the sample loading in 0.5 ml of 6
207 M HCl. The matrix species were eluted in 3 ml of the same acid and, subsequently, Fe was
208 quantitatively eluted with 2 ml of 0.05 M HCl. The purified Fe solutions were evaporated at 120°C.
209 After evaporation, purified Fe samples were redissolved in a 0.05 M HCl solution that was used for
210 the MC-ICP-MS analysis. Iron and the internal standard, Ni, were set to concentration producing
211 signals of ca. 40 V of ^{56}Fe and 20V for ^{60}Ni. Iron isotope measurements were performed at the
212 CNRS-INSU National MC-ICP-MS facility in Lyon using a Thermo Electron Neptune Plus and at
213 GET-CNRS in Toulouse using a Thermo Electron Neptune MC-ICP-MS (Bremen, Germany)[49]. All
214 analyses are reported in the delta notation relative to the IRMM-014 standard, expressed as $\delta^{57}Fe$,
215 which represents the deviation in per mil relative to the reference material:

216 $$\delta^{57}\mathrm{Fe}\ (‰) = \left(\frac{(^{57}Fe/^{54}Fe)_{sample}}{(^{57}Fe/^{54}Fe)_{IRMM14}} - 1\right) * 1000$$

217 We also obtained $\delta^{56}Fe$ values but, since the relationships between $\delta^{56}Fe$ and $\delta^{57}Fe$ of the
218 samples plot on a single mass fractionation line ($\delta^{57}Fe = 1.466 \times \delta^{57}Fe + 0.005$, $R^2 = 0.9995$, $p <$
219 10^{-4}), only $\delta^{57}Fe$ values are discussed in this paper. Data quality was checked by the analysis of our

220 in-house hematite standard every 5 samples in the analytical sequence. Our mean value of
221 0.771±0.047‰ (2SD) for this standard obtained between Lyon and Toulouse from pooling 51
222 individual analyses by groups of 6 was consistent with the values of 0.766±0.072‰ reported
223 previously[8].
224
225 **3. Results and Discussion**
226 *3.1. Iron in the < 0.22 μm fraction during biodegradation experiments: Heavier isotopes*
227 *adsorption onto and lighter isotopes uptake by live cells of P. aureofaciens*
228 The studied surface waters were oxygenated, organic- and Fe-rich (pH = 7.1, DOC = 12 mg
229 L^{-1}, Fe = 208 μg L^{-1} in KAR-1; pH = 5.4, DOC = 38.7 mg L^{-1}, and Fe = 4310 μg L^{-1} in ZPBL). The
230 stream water contained ~24% of Fe(II) and the fen contained ~20% of Fe(II); the $LMW_{< 1\ kDa}$
231 fraction of DOC was sizably higher in the stream compared to the fen (77 and 29%, respectively).
232 The experimental results are reported in **Table 1** whereas those of the control experiments are listed
233 in **Table S1**. The pH value increased by 0.6 and 1.2 unit over 4 days of *P. aureofaciens* reaction
234 with stream water and fen water, respectively (**Table 1**). There was no sizeable DOC decrease over
235 the first 1 h of reaction. The long-term removal (1 – 100 h) of DOC by *P. aureofaciens* was not
236 pronounced in the stream water but was high in the fen water (-33±5%).
237 Iron exhibited initial adsorption after 1 h of reaction as it is seen from the difference between
238 the stream and the fen water control and bacterial suspension at the beginning of experiment (**Fig. 2**
239 **A and B and Table 1**). The proportions of fast adsorption (0-1 h) and intracellular
240 assimilation/Fe(III) hydroxide (1-93 h) relative to total Fe removal in the experiments were
241 respectively equal to 35% and 37% in the stream water and 30% and 25% in the fen water. In the
242 latter, the concentration of divalent Fe decreased almost 3-fold over the first day of reaction relative
243 to control (**Fig. 2 C**). No sizeable change of Fe(II) in stream water could be assessed because the
244 Fe(II) concentration in KAR-1 (not shown) was 30±20 μg/L (~16% of total dissolved Fe), with a
245 quantification limit of Fe(II) by this method of 15 μg/L[45].

All initial solutions were undersaturated with respect to Fe-bearing minerals. Calculated change of Fe(II) and Fe(III) speciation in the course of experiments demonstrated the dominance of Fe(III)-fulvic acid (FA) complexes. The Fe(II) bound to FA fully disappeared in the stream and decreased by a factor of 3 in the fen waters (**Fig. S1**). Specifically, the Fe(III) complex with carboxylic groups of FA degraded 4-fold in both fen and stream water, whereas phenolic complex of Fe(III) remained stable (**Table S2**). The proportion of Fe(II) complex with carboxylates of FA increased whereas Fe(II)-weak electrostatic complex completely disappeared. This is consistent with highly reactive behavior of dissolved Fe(II) in biodegradation experiments.

The second < 0.22 µm filtration step in the laboratory of the control water samples showed that the 6 months storage in the fridge did not affect stream water chemical composition but it induced a decrease of Fe concentration in the fen water from 4310 µg/L to 2470 µg/L, accompanied by a change in δ^{57}Fe from 0.25±0.06‰ to 1.06±0.04‰. A strong δ^{57}Fe increase from 1.59±0.05‰ to 2.87±0.07‰ also resulted from the storage for the stream water (Table 1 and S1). This change could be linked to some $Fe(OH)_3$ precipitation due to either aggregation of Fe(III)-rich organic colloids or Fe(II) oxidation. To preserve at least the Fe isotopic composition of DOC-rich waters over several months, immediate freezing after filtration in the field on the sampling site is preferable[50], but this is not always possible for logistical reasons.

Although the fractionation of Fe between bacterial cells and organo-ferric colloids has not been studied previously, the adsorption of metal cations such as Zn^{2+} at the microorganism cell surface is known to favor the heavier isotopes[51] and both Fe^{2+} and Fe^{3+} ions follow this rule[30,31]. The heavier Fe isotopes are preferentially adsorbed onto solid surfaces during equilibrium isotope fractionation processes[36]. Experiments that lasted 11 days with anaerobic phototrophic Fe-oxidizing, aerobic neutrophilic Fe-oxidizing, and heterotrophic Fe-reducing bacteria demonstrated that metabolically-produced hydrous ferric oxide (HFO) exhibited heavier isotopic composition than the initial Fe(II), with a fractionation factor (Δ^{57}Fe) of +2.2±0.3‰[52]. Further, depending on the phytoplankton species and the composition of the culture medium, the cell surface was found to be enriched in heavier

isotopes by +2.4±0.6 ‰ to +2.9±0.1 ‰ for Fe^{2+} containing solution and by +0.4±0.2 to +1.0±0.2 ‰ for Fe^{3+} solution[30]. More recent measurements of Fe isotope fractionation during Fe adsorption onto phytoplankton cells quantitatively confirmed these data[31]. The value $\Delta^{57}Fe_{cell\text{-}solution}$ of +0.5±0.1‰ for the river water inferred from the present study suggests essentially Fe^{3+} ion adsorption onto *P. aurefaciens* cell surfaces, presumably forming Fe(III)-phosphoryl complexes[44]. Note however that the competition between surface organic moieties and aqueous organic complexes for heavy Fe isotopes can decrease the magnitude of isotopic offset in humic waters compared to experimental solutions with low DOC. At present, the isotopic offset for adsorption of organo-ferric colloids onto organic surfaces is not known and this should be the subject of future research.

The interaction of stream water with heterotrophic bacterium produced first, a drop in $\delta^{57}Fe$ of ca 0.4‰ in solution due to adsorption of heavier isotopes on the cell surface, and then a gradual increase in aqueous $\delta^{57}Fe$ from +2.5±0.1‰ to +3.2±0.1‰ between 1 and 24 h (**Fig. 3 A**) yielding $\Delta^{57}Fe_{cell\text{-}solution}$ of -0.7‰. This implies removal of lighter Fe isotopes due to their preferential intracellular uptake. After an initial drop in the stream water $\delta^{57}Fe$, the long-term removal of lighter Fe isotopes by live bacteria produced ca 0.7‰ increase in $\delta^{57}Fe$ over the first 20 h of reaction that remained constant to 50 h (**Fig. 3A**). This strongly supports biological mechanism of lighter Fe isotopes uptake inside cells rather than metabolically-induced $Fe(OH)_3$ precipitation. In the latter case, the solid phase would be enriched in heavy isotope ($\Delta^{57}Fe_{FeOOH\text{-}Fe(aq)}$ = +1.5 to +4-5‰)[32,53,54] as also supported by natural observations[9,53]. The present result is at variance with previous Fe assimilation by magnetotactic bacteria[33] or phytoplankton[42] that inferred a heavier Fe isotope uptake inside the cells due to a combined Fe oxidation. However, the Fe(III)-DOM complexes in solution retain heavy isotope as it is known for $Fe^{3+}(H_2O)_6$ –Fe(III) chelate (DFO-B): the organic complexes are enriched in heavy isotopes with an isotopic offset of +0.90±0.23 ‰[55], and overall, there is a strong positive correlation between Fe fractionation factors and the Fe-binding affinity of the ligands[56]. According to vMinteq calculation, the majority of Fe in our experimental solutions was bound to phenolic complexes with fulvic acids (Fig. S1, Table S2). Therefore, we suggest that strong

298 complexation of isotopically heavy Fe(III) with DOM prevents the intracellular uptake of heavier Fe
299 isotopes.

300 In the fen water, we observed a similar $\delta^{57}Fe$ evolution during biodegradation experiments,
301 though with smaller variations. The isotopic composition of dissolved Fe did not appreciably change
302 during *P. aureofaciens* short-term interaction with fen water: we observed only weak adsorption of
303 heavy isotope (<0.1‰) and a weak assimilation of light isotopes $\Delta^{57}Fe_{cell\text{-}solution} \leq 0.1‰$ over first 40
304 h (**Fig. 3 B**). Relative to the sterile control, a decrease in $\delta^{57}Fe$ at the beginning of experiment
305 signified preferential adsorption of heavy isotopes with $\Delta^{57}Fe_{cell\text{-}solution} = +0.2\pm0.1‰$. Over 100 h of
306 reaction, light Fe isotopes were taken up by the cells as the $\delta^{57}Fe$ of solution increased from
307 +0.86±0.1‰ to +1.05±0.05‰.

308 Overall, the effect of bio-transformation of Fe isotopic signature were much stronger in the
309 stream water compared to the fen water, which may be due to different concentration of Fe in these
310 two samples (200 and 4300 µg/L) at otherwise similar bacterial concentration ($1g_{wet}$/L). As a result,
311 there was an order of magnitude higher ligand : metal ratio ((cell surface sites) : Fe fraction) in the
312 stream compared to the fen water.

313

314 *3.2. Iron concentrations and isotopic signatures evolution during photodegradation of organo-ferric*
315 *colloids: Removal of heavier isotopes due to Fe(III) hydroxide formation and appearance of*
316 *isotopically light Fe(II) in the LMW fraction*

317 There was no pH variation in the course of photodegradation experiments: within the uncertainty
318 of duplicates (< 0.1-0.2 pH unit), the pH in the dark control and the light experiment was identical
319 and equal to 7.0±0.2 and 5.3±0.1 in the stream and fen water, respectively (Table 1 and S1). The
320 DOC concentration in <0.22 µm fraction of stream and fen water decreased by 30 and 50%,
321 respectively, over 200 to 250 h of photodegradation experiment (Table 1). There was a good
322 correlation between ultraviolet absorbency ($UV_{254\ nm}$) and Fe concentration in the fen water (R^2 =
323 0.928) which was absent in the stream water in the course of experiment (R^2 = 0.19).

In the stream water, Fe concentration remained generally constant within the uncertainties over 250 h of exposure to sunlight, relative to the dark control, and no formation of flocculent material was noted (**Fig. 4 A).** There was 50 to 80% removal of Fe(II), between 110 and 250 h of exposure, which occurred for both <0.22 µm and <10 kDa fractions (from 50 to 15 µg/L and from 20 µg/L to < limit of quantification, respectively, **Fig. 4 B**).

The removal of Fe during fen water exposure to sunlight was strong in the < 0.22 µm fraction (~ -75% of initial concentration) and did not occur in the < 10 kDa fraction (≤7% of the initial concentration, **Fig. 4 D and Table 1**). A notable increase in total Fe concentration (ca. 210%) in the $LMW_{<1\ kDa}$ fraction was observed over 200 h of exposure (**Fig. 4 D**). The divalent Fe concentration decreased by 50% in the < 0.22 µm fraction but strongly increased (~500%) in the < 1 kDa fraction (**Fig. 4 E and Table 1**). Over 196 h of irradiation, the Fe(II) proportion increased from 20 to 50% in the < 0.22 µm fraction and from 35 to 55% in the < 1 kDa fraction. The <10 kDa fraction did not demonstrate any difference in Fe(II) concentration between the sunlight-irradiated samples and the dark control.

During sunlight exposure, the < 0.22 µm fraction of the fen water became depleted in Fe as the molar ratio of C_{org}:Fe increased from 50 to 100, as can be calculated from evolution of concentrations listed in Table 1. This trend mainly stems from more efficient Fe removal compared to DOC. The change of this ratio in the stream water was within the experimental uncertainty. The C_{org}:Fe ratio in the fen water colloids (1 kDa – 0.22 µm) did not change in the course of photo-degradation, from 31 at the beginning of experiment to 32 after 193 h of sunlight exposure. In the $LMW_{<1kDa}$ fraction of fen water, the C_{org}:Fe ratio decreased from 247 to 126.

All size fractions of the initial stream solution and the $LMW_{<1\ kDa}$ fraction of the fen water were undersaturated with respect to Fe-bearing minerals. The initial < 0.22 µm fen water was supersaturated with respect to goethite, lepidocrocite and magnetite (Saturation Indexes = 1.3, 0.62, and 3.6, respectively). The speciation calculation using vMinteq also demonstrated that Fe(III) is fully complexed with DOM (**Fig. S2**). Therefore, the removal of Fe in the form of particulate Fe

hydroxide could be only due to liberation of part of Fe from organic complexes after photolytic degradation of colloidal DOM that stabilized Fe (III) polymers in solutions. Calculated Fe(II) and Fe(III) speciation in the fen water before and after photodegradation experiment demonstrated an appearance of ~2% of inorganic Fe(II) and approx. 2-fold increase of Fe(II) bound to DOM, in both < 0.22 μm and < 1 kDa size fraction (**Fig. S2**). In the stream water, there was a 3-fold decrease of Fe(II) bound to DOM. Specifically, the Fe(III) complex with carboxylic groups of FA decreased and increased 3-fold in fen and stream waters, respectively (**Table S3**). Phenolic complexes of Fe(III) which accounted for >93…99% of all Fe, remained constant in the course of experiment. In the fen water, the proportion of Fe(II)-weak electrostatic complex strongly decreased (by a factor of 4.5 and 1.5 in < 0.22 μm and < 1 kDa fractions, respectively) whereas Fe(II) complex with FA carboxylates increased in < 0.22 μm fraction and stayed constant in < 1 kDa fraction (**Table S3**). According to vMinteq predictions, 4.5×10^{-5} M of ferrihydrite should could have precipitated from the fen water over 200 h of solar irradiation. This is equivalent to ~2250 μg/L of dissolved Fe concentration decrease, which is comparable to the range encountered in the experiment (ca. 3400 μg/L, see **Fig. 4 D** and **Table 1**).

The isotopic signature of stream water samples remained constant in the < 0.22 μm fraction of dark control and sun-light irradiated quartz reactors (**Fig. 5A**). The δ^{57}Fe value of the < 10 kDa fraction decreased from +2.93±0.05‰ to +1.92±0.1‰ after first 110 h of exposure and then remained constant. Note that the initial < 10 kDa fraction of stream water was ca. 1.5 ‰ isotopically heavier than the < 0.22 μm fraction, in agreement with previous measurement of Fe isotopic composition in colloids of Northern Karelian streams[37].

The isotopic ratio in the dark control of fen water remained stable at δ^{57}Fe = 0.2±0.3‰, except in the $LMW_{< 1\ kDa}$ fraction, where a +0.6‰ increase was observed, related to the Fe and DOC loss (Table S1). Similar effect was reported in the organic-rich Negro River where it was attributed to the loss of isotopically light aggregates of Fe(III) with OM[50]. In contrast to dark controls, sunlight irradiation of the fen water strongly impacted δ^{57}Fe in all 3 fractions, <0.22 μm, <10 kDa and <1

kDa (**Fig. 5 B**). Over first 100 h of reaction, there was sizeable, from 1 to 2‰, decrease of δ^{57}Fe in the <0.22 μm and the <1-10 kDa fraction, respectively. Over the next 100 h, the δ^{57}Fe further decreased by 1.5 ‰ in the <0.22 μm fraction and stabilized at δ^{57}Fe = -2.2±0.2‰ in the <1 and <10 kDa fractions.

Sunlight exposure of stream water did not produce any sizable change of Fe concentration and isotopic signature in the < 0.22 μm fraction (**Fig. 4A** and **5A**), in general agreement with stability of boreal high latitude metal concentration in riverwaters with respect to sunlight irradiation[28,57]. After 100 h of sunlight irradiation, the < 10 kDa fraction of stream water became 1.5‰ lighter compared to the initial value or the dark control (**Fig. 5A**), although the Fe concentration in this fraction decreased only between 100 and 250 h of exposure (**Fig. 4 A**). A plausible explanation for this isotopic pattern invokes the presence of strong low molecular weight (< 10 kDa) Fe(III)-organic ligand (chelate) complexes which are enriched in heavy isotopes[55] and which are capable to stabilize dissolved Fe. For example, aquatic prokaryotes produce the LMW (0.3 – 1 kDa) Fe(III) siderophores[58]. These light sensitive, presumably aromatic Fe complexes represent a small iron fraction of overall $Fe_{<10\ kDa}$ pool, but our results indicate that it exhibits a very high δ^{57}Fe value. The isotopic signature of $LMW_{<1\text{-}10\ kDa}$ Fe poor, C-rich fraction of Karelian waters reaches +4.2‰[37]. We hypothesize that these isotopically heavy Fe-organic complexes have low residence time in the river channel and are produced due to periphyton or plankton metabolic activity.

The Fe in the fen water was strongly sensitive to sunlight irradiation as > 70% Fe was removed from the <0.22 μm fraction and all filtrates and ultrafiltrates became strongly impoverished in heavy isotopes (**Fig. 4 D, 5 B**). The removal of Fe followed that of $SUVA_{254}$ decrease[28], suggesting that the majority of Fe that is removed from the fen water was bound to aromatic (colored) organic carbon. This is also confirmed by the dominance of Fe(III)-phenolic groups of FA in Fe speciation (**Table S3**). It is possible that the photolysis of Fe-DOM complexes liberates ionic Fe which could be removed from solution in the form of isotopically heavy Fe hydroxides. The removal of heavy isotopes by sunlight oxidation of organo-ferric colloids observed in this study (+2.3±0.1‰) is

generally consistent with known fractionation of Fe between Fe(III) hydroxide and Fe(II) solution: ($\Delta^{57}Fe_{FeOOH\text{-}Fe(aq)}$ = +2.3±0.3‰, ref. 52-54).

In contrast to what was hypothesized in our earlier work on these waters[37], no enrichment in heavy isotopes of LMW fraction was observed during photolysis of humic waters. Here we suggest that Fe(II) generated in the < 1 kDa fraction is enriched in light isotopes compared with initial Fe(III) in colloids, thus producing overall negative δ^{57}Fe value in $LMW_{< 1\ kDa}$ after irradiation. Assuming an equilibrium fractionation factor between Fe(II) and Fe(III) of -4.3‰[59] and considering the starting water δ^{57}Fe close to 0‰ (**Fig. 5B**), the 55% of Fe(II) in < 1 kDa fraction (**Fig. 4 F**) provides 0.55×(-4.3‰) = -2.4‰ of δ^{57}Fe, in full agreement with values shown in **Fig. 5 B**. This <0.22 μm fraction comprises two Fe pools: (1) Fe remaining after Fe^{2+}(aq) → $Fe(OH)_3$ and after Fe^{3+}(colloidal) → $Fe(OH)_3$ precipitation, and (2) isotopically light Fe^{2+} produced in the LMW fraction. It is important to note that the photolysis of organo-ferric colloids which represents 80% of Fe in <0.22 μm fraction, removes Fe(III) in the form of $Fe(OH)_3$ hydroxides corresponding to $\Delta^{57}Fe_{Fe(III)hydroxide\text{-}Fe(aq)}$ of 2.4±0.1‰, **Fig 5B**. The observed enrichment of solid phase in heavier isotopes is therefore much lower than Fe^{2+}(aq) → $Fe(OH)_3$ reaction ($\Delta^{57}Fe_{Ferrihydrite\text{-}Fe(II)}$ = 4.7 ‰[39]) and opposite in sign to Fe^{3+}(aq) → $Fe(OH)_3$ reaction ($\Delta^{57}Fe_{Fe(III)hydroxide\text{-}Fe(aq)}$ = -0.9 ‰[60]). Lower value of isotopic enrichment compared to the equilibrium fractionation factor between Fe(II)aq and pure ferrihydrite[39] may be due to Fe(II) sorption onto hydrous Fe(III)-oxides and subsequent atom (isotope) exchange between Fe(II) and hydrous Fe(III)-oxides. These processes are known to be responsible for substantial Fe isotope fractionation in a number of organic-free systems[36, 61-64]. However, in humic waters, both remaining $Fe(II)_{aq}$ ions and >FeOOH surface sites of newly precipitated Fe(III) hydroxides are likely to be bound to carboxylic and phenolic groups of fulvic acids. Organic matter associated with Fe(III) hydroxide and surface organic - Fe complexes may modify the magnitude of Fe(II)-Fe(III) hydroxide isotope exchange[34]. Thus, Chanda et al[65] argued that the presence of organic C causes distortion of the Fe octahedral structure and decreases by ca. 1.2 ‰ ($^{57}Fe/^{54}Fe$) the fractionation factor between Fe(II) and NOM-ferrihydrite. Similar mechanisms may operate in case

428 of isotopic exchange between Fe(II) and organo-ferric aggregates produced by photolysis of Fe(III)-
429 rich colloids.

430 We observed notable differences in the degree of Fe concentrations and Fe isotopic
431 composition during photolysis of the fen and the stream water. These differences may stem from the
432 combination of two main factors controlling the degree of DOM and Fe photo-reactivity in natural
433 waters: the fen water is a 1.5 unit of pH lower than the stream and has a factor of 30 higher in Fe
434 concentration. The water acidity is known to exert a strong positive effect on the photolysis of
435 DOM[65,66] and the DOM photobleaching is enhanced by elevated Fe concentration via the photo-
436 Fenton effect below pH 6[67]. Overall, in natural settings, one may expect large variation of Fe and
437 DOM photo-liability depending on the environmental context. Thus, slightly alkaline (pH = 8)
438 surface water from a temperate peatland in China exhibited quite higher photo-stability of Fe[68],
439 whereas acidic DOC-rich waters from a subtropical swamp under UV irradiation demonstrated 10
440 times more efficient removal of Fe relative to DOC[69]. As such, depending on the lithological context
441 of peatlands (i.e., acidic (felsic) or carbonate (sedimentary) rocks), the degree of Fe chemical and
442 isotopic composition change under sunlight may be dramatically different.
443
444 *3.3. Complexity of Fe isotope fractionation in boreal humic waters and implication for inland*
445 *waters Fe isotope budget*

446 We hypothesize several processes responsible for chemical removal and isotopic redistribution of
447 Fe among different colloidal pools in DOM- and Fe-rich stream and fen water, shown schematically
448 in **Fig. 6.** High molecular size (10 kDa – 0.45 μm) organo-ferric colloids representing the majority of
449 dissolved (<0.22 μm) Fe[17,37] are stabilized by organic ligands originating from topsoil and bog peat
450 leaching. In addition, a small fraction of Fe(III) could be linked to highly specific, $LMW_{<1\text{-}10\ kDa}$
451 ligands having a short residence time in the river channel; these complexes could be produced via in-
452 stream plankton and periphyton activity. In the fen water, a sizeable fraction of Fe is in the form of
453 Fe(II) inorganic and organic complexes[70]. In the river water, the HMW colloids are subjected to

biologically-controlled transformations via *i*) adsorption onto surfaces of aquatic bacteria, favoring heavier isotopes to the cells, with an overall $\Delta^{57}Fe_{cell\ ads\text{-}solution}$ = +0.4±0.1‰, and *ii*) assimilation by live bacteria, favoring lighter Fe isotopes to the cells with $\Delta^{57}Fe_{cell\ incorp\text{-}solution}$ = -0.7±0.1‰. On a short-term scale (hours), the humic waters, once placed in contact with bacteria, are therefore becoming enriched in lighter Fe isotopes, followed, on a long-term scale (days), by enrichment in heavier Fe isotopes. Considering available data on preferential heavy isotope adsorption onto phytoplanktonic and peryphytic cyanobacteria inhabiting natural waters (from +0.4 to +2.9‰, ref. 30), and neglecting Rayleigh distillation processes given that we are dealing with open systems (hydrological continuum, ref. 17), the overall magnitude of diurnal variation of dissolved (< 0.45 μm) δ^{57}Fe in small streams and stagnant surface waters in the presence of common soil bacteria may range from +2.7‰ to +0.7‰. This greatly exceeds the range of Fe isotopic excursions in various sediments and in all possible bedrocks[71].

Further, photolysis of DOM and Fe-DOM complexes in surface waters, which operates at the time scale comparable to water and solute residence time in these waters (1-10 days), is capable to dramatically enrich in lighter Fe isotopes (by 1.5 to 2.5‰) of both dissolved (<0.22 μm) and $LMW_{<1\text{-}10\ kDa}$ water fraction. We suggest that the two major processes of organo-ferric colloid transformation under sunlight in natural waters include: (*i*) degradation of the organic part of colloids (1 kDa – 0.22 μm) and production of low molecular weight (< 1 kDa) organic ligands including carboxylic and aromatic chelates capable of strong binding of Fe ions; (*ii*) aggregation of HMW organo-ferric colloids and precipitation of Fe-rich oxy(hydroxide) after the solar radiation-induced removal of stabilizing organic matter.

The enigmatic enrichment of the LMW fraction (<1-10 kDa) of the stream water in heavy isotopes[37] is therefore most likely linked to strong, presumably aromatic, isotopically heavy Fe(III)-organic complexes. These compounds have low residence time and are produced in the river channel due to periphyton or plankton metabolic activity. In addition, sunlight irradiation of subarctic humic waters may produce 10-fold increase in aliphatic and aromatic carbonic acids[72] capable to bind both

Fe(II) and Fe(III). Altogether, bio- and photo-degradation of dissolved Fe in river, stream and bog waters can produce from -2 to +3 ‰ δ^{57}Fe variation on time scales of a few days. Because this time is generally shorter than the water residence time in surface waters, considering of Fe isotopic signature of rivers and streams as a conservative value inherited from soils and using it for tracing the sources and weathering regime on watersheds are not warranted at short time- and length-scales. Therefore, naturally-induced variations in biological activity (switching from heterogenic bacteria uptake to adsorption onto aquatic phototrophs) and sunlight illumination can modify the overall Fe isotopic signatures of surface waters by several permil. Moreover, when considering the processes responsible for Fe chemical and isotopic transformation in organic-rich streams, one has to assess both dissolved (<0.45 or <0.22 μm) and $LMW_{< 1\text{-}10\ kDa}$ fractions of metal, since their isotopic signatures and photo-susceptibility may be dramatically (by 1 to 3‰) different.

Acknowledgements

We acknowledge support from a RFBR research projects № 17-05-00342_a, and 18-05-00162, and the CNRS (PRC) No 1070 project. We thank P. Télouk in Lyon and J. Chmeleff in Toulouse for maintaining the MC-ICP-MS instruments in good working order, and M. Henri for maintaining the clean room in Toulouse.

References

(1) Beard, B.L.; Johnson, C.M.; Von Damm, K.L.; Poulson, R.L. Iron isotope constraints on Fe cycling and mass balance in oxygenated Earth oceans. *Geology* **2003**, *31*, 629-632.

(2) Labatut, M.; Lacan, F.; Pradoux, C.; Chmeleff, J.; Radic, A.; Murray, J.W.; Poitrasson, F.; Johansen, A.M.; Thil, F. Iron sources and dissolved-particulate interactions in the seawater of the Western Equatorial Pacific, iron isotope perspectives. *Global Biogeochem. Cycles* **2014**, *28*, 1044-1065.

(3) Ingri, J.; Malinovsky, D.; Rodushkin, I.; Baxter, D.C.; Widerlund, A.; Andersson, P.; Gustafsson, O.; Forsling, W.; Ohlander, B. Iron isotope fractionation in river colloidal matter. *Earth Planet. Sci. Lett.* **2006**, *245* (3-4), 792-798.

(4) Ingri, J.; Conrad, S.; Lidman, F.; Nordblad, F.; Engstrom, E.; Rodushkin, I.; Porcelli, D. Iron isotope pathways in the boreal landscape: Role of the riparian zone. *Geochim. Cosmochim. Acta* **2018**, *239*, 49-60.

(5) Escoube, R.; Rouxel, O.; Pokrovsky, O.S.; Schroth, A.; Holmes, R.M.; Donard, O.F.X. Iron isotope systematics in Arctic rivers. *Comptes Rendus Geoscience* **2015**, *347* (7-8), 377-385; DOI 10.1016/j.crte.2015.04.005.

(6) Conrad, S.; Ingri, J.; Gelting, J.; Nordblad, F.; Engström, E.; Rodushkin, I.; Andersson, P.S.; Porcelli, D.; Gustafsson, Ö.; Semiletov, I.; Öhlander, B. Distribution of Fe isotopes in particles and

colloids in the salinity gradient along the Lena River plume, Laptev Sea. *Biogeosciences,* **2019,** 16, 1305-1319, https://doi.org/10.5194/bg-16-1305-2019.

(7) Chen, J.B.; Busigny, V.; Gaillardet, J.; Louvat, P.; Wang, Y.N. Iron isotopes in the Seine River (France): Natural versus anthropogenic sources. *Geochim. Cosmochim. Acta* **2014**, *128*, 128-143.

(8) Poitrasson, F.; Vieira, L.C.; Seyler, P.; dos Santos Pinheiro, G.M.; Mulholland, D.S.; Bonnet, M.P.; Martinez, J.M.; Lima, B.A.; Allard, T.; Boaventura, G.R.; Chmeleff, J.; Dantas, E.; Guyot, J.L.; Mancini, L.; Pimentel, M.M.; Santos, R.V.; Sondag, F.; Vauchel, P. Iron isotope composition of the bulk waters and sediments from the Amazon River Basin. *Chem. Geol.* **2014**, *377*, 1-11.

(9) Song, L.; Liu, C.-Q.; Wang, Z.-L.; Zhu X.; Teng, Y.; Liang, L.; Tang, S.; Li, J. Iron isotope fractionation during biogeochemical cycle: information from suspended particulate matter (SPM) in Aha Lake and its tributaries, Guizhou, China. *Chem. Geol.* **2011**, *280* (1–2), 170–179.

(10) Busigny, V.; Planavsky, N.J.; Jezequel, D.; Crowe, S.; Louvat, P.; Moureau, J.; Viollier, E.; Lyons, T.W. Iron isotopes in an Archean ocean analogue. *Geochim. Cosmochim. Acta* **2014**, *133*, 443-462.

(11) Serikova, S.; Pokrovsky, O.S.; Ala-aho, P.; Kazantsev, V.; Kirpotin, S.; Kopysov, S.; Krickov, I.; Laudon, H.; Manasypov, R.M.; Shirokova, L.S.; Soulsby, C.; Tetzlaff, D.; Karlsson, J. High riverine CO_2 emissions at the permafrost boundary of Western Siberia. *Nature Geoscience* **2018**, *11,* 825-829.

(12) Serikova, S., Pokrovsky, O.S., Laudon, H., Krickov, I.V., Lim, A.G., Manasypov, R.M., Karlsson, J. High carbon emissions from thermokarst lakes of Western Siberia. *Nature Comm.,* **2019,** *10,* Art No 1552. https://doi.org/10.1038/s41467-019-09592-1.

(13) Kritzberg, E.S.; Villanueva, A.B.; Jung, M.; Reader, H.E. Importance of boreal rivers in providing iron to marine waters. *PLoS ONE* **2014**, *9*, e107500, DOI 10.1371/journal.pone.0107500.

(14) Hirst, C.; Kutscher, L; Murphy, M; Shaw, S.; Burke, I.T.; Kaulich, B.; Maximov, T.; Pokrovsky, O.S.; Mörth, C.-M; Andersson, P.S.; Porcelli, D. Characterization and stability of Fe-bearing particles in the Lena River catchment, NE Russia. *Geochim. Cosmochim. Acta* **2017**, *213*, 553–573.

(15) Hassellov, M.; Von Der Kammer, F. Iron oxides as geochemical nanovectors for metal transport in soil–river systems. *Elements* **2008**, *4* (6), 401–406.

(16) Vonk, J.E.; Tank, S.E.; Bowden, W.B.; Laurion, I.; Vincent, W.F.; Alekseychik, P.; Amyot, M.; Billet, M.F.; Canário, J.; Cory, R.M.; Deshpande, B.N.; Helbig, M.; Jammet, M.; Karlsson, J.; Larouche, J.; MacMillan, G.; Rautio, M.; Walter Anthony, K.M.; Wickland, K.P. Reviews and Syntheses: Effects of permafrost thaw on Arctic aquatic ecosystems. *Biogeosciences* **2015**, *12*, 7129-7167.

(17) Ilina, S.M.; Lapitsky, S.A.; Alekhin, Y.V.; Viers, J.; Benedetti, M.; Pokrovsky, O.S. Speciation, size fractionation and transport of trace element in the continuum soil water – mire – lake – river – large oligotrophic lake of a subarctic watershed. *Aquat. Geochem.* **2016**, *22* (1), 65-95.

(18) Shirokova, L.S.; Bredoire, R.; Rolls, J.-L.; Pokrovsky, O.S. Moss and peat leachate degradability by heterotrophic bacteria: fate of organic carbon and trace metals. *Geomicrobiology J.* **2017**, *34* (8), 641-655.

(19) Kopacek, J.; Klementova, S.; Norton, S.A. Photochemical production of ionic and particulate aluminum and iron in lakes. *Environ. Sci. Technol.* **2005,** *39,* 3656–3662.

(20) Shiller, A.M.; Duan, S.; van Erp, P.; Bianchi, T.S. Photo-oxidation of dissolved organic matter in river water and its effect on trace element speciation. *Limnol. Oceanography* **2006,** *51*(4), 1716–1728

(21) Mann, P.J.; Sobczak, W.V.; LaRue, M.M.; Bulygina, E.; Davydova, A.; Vonk, J.E.; Schade, J.; Davydov, S.; Zimov, N.; Holmes, R.M.; Spencer, R.G.M. Evidence for key enzymatic controls on metabolism of Arctic river organic matter. *Global Change Biol.* **2014**, *20* (4), 1089-1100.

(22) Vähätalo, A.V.; Salonen, K.; Münster, U.; Järvinen, M.; Wetzel, R.G. Photochemical transformation of allochthonous organic matter provides bioavailable nutrients in a humic lake. *Acta Hydrobiol.* **2003**, *156*, 287-314.

(23) Kelton, N.; Molot, L.A.; Dillon, P.J. Effect of ultraviolet and visible radiation on iron lability in boreal and artificial waters. *Aquat. Sci.* **2007**, 69, 86–95.

(24) Garg, S.; Ito, H.; Rose, A.L.; Waite, T.D. Mechanism and kinetics of dark iron redox transformations in acidic natural organic matter solutions. *Environ. Sci. Technol.* **2013**, *47*, 1861-1867.

(25) Blazevic, A.;, Orlowska, E.; Kandioller, W.; Jirsa, F.; Keppler, B.K.; Tafili-Krueziu, M.; Linert, W.; Krachler, R.F.; Krachler, R.; Rompel, A. Photoreduction of terrigenous Fe-humic substances leads to bioavailable iron in oceans. *Angew. Chem. Int. Ed*. **2016**, *55*, 6417-6422.

(26) Oleinikova, O.V.; Shirokova, L.S.; Drozdova, O.Yu.; Lapitskiy, S.A.; Pokrovsky, O.S. Low biodegradability of dissolved organic matter and trace metals from subarctic waters. *Sci. Total Env.* **2018**, *618*, 174-187.

(27) Oleinikova, O.V.;Shirokova, L.S.; Gérard, E.; Drozdova, O.Yu; Lapitskiy, S.A.; Bychkov, A.Yu; Pokrovsky, O.S. Transformation of organo-ferric peat colloids by a heterotrophic bacterium. *Geochim. Cosmochim. Acta* **2017**, *205*, 313-330.

(28) Oleinikova, O.V.; Drozdova, O.Yu; Lapitskiy, S.A.; Demin, V.V.; Bychkov, A.Yu; Pokrovsky, O.S. Dissolved organic matter degradation by sunlight coagulates organo-mineral colloids and produces low-molecular weight fraction of metals in boreal humic waters. *Geochim. Cosmochim. Acta* **2017**, *211*, 97-114.

(29) Beard, B.L.; Johnson, C.M.; Cox, L.; Sun, H.; Nealson, K.H.; Aguilar, C. Iron isotope biosignatures. *Science* **1999**, *285* (5435), 1889-1892.

(30) Mulholland, D.S.; Poitrasson, F.; Shirokova, L.S.; Gonzalez, A.; Pokrovsky, O.S.; Boaventura, G.R.; Vieira, L.C. Iron isotope fractionation during Fe(II) and Fe(III) adsorption on cyanobacteria. *Chem. Geol.* **2015**, *400*, 24-33.

(31) Swanner, E.D.; Bayer, T.; Wu, W.; Hao, L.; Obst, M.; Sundman, A.; Byrne, J.M.; Michel, F.M.; Kleinhanns, I.C.; Kappler, A.; Schoenberg, R. Iron isotope fractionation during Fe(II) oxidation mediated by the oxygen-producing marine cyanobacterium *Synechococcus* PCC 7002. *Environ. Sci. Technol.* **2017**, *51* (9), 4897-4906.

(32) Swanner, E.D.; Wu, W.; Schoenberg, R.; Byrne, J.; Michel, F.M.; Pan, Y.; Kappler, A. Fractionation of Fe isotopes during Fe(II) oxidation by a marine photoferrotroph is controlled by the formation of organic Fe-complexes and colloidal Fe fractions. *Geochim. Cosmochim. Acta* **2015,** *165*, 44-61.

(33) Amor, M.; Busigny, V.; Louvat, P.; Tharaud, M.; Gelabert, A.; Cartigny, P.; Carlut, J.; Isambert, A.; Durand-Dubief, M.; Ona-Nguema, G.; Alphandery, E.; Chebbi, I.; Guyot, F. Iron uptake and magnetite biomineralization in the magnetotactic bacterium Magnetospirillum magneticum strain AMB-1: An iron isotope study. *Geochim. Cosmochim. Acta* **2018**, *232*, 225-243.

(34) Zhou, Z.; Latta, D.E.; Noor, N.; Thompson, A.; Borch, T.; Scherer, M.M. Fe(II)-catalyzed transformation of organic matter-ferrihydrite coprecipitates: A closer look using Fe isotopes. *Environ. Sci. Technol.* **2018,** *52,* 11142-11150.

(35) Brantley, S.L.; Liermann, L.J.; Guynn, R.L.; Anbar, A.; Icopini, G.A.; Barling, J. Fe isotopic fractionation during mineral dissolution with and without bacteria. *Geochim. Cosmochim. Acta* **2004**, *68*, 3189-3204.

(36) Crosby, H.A.; Johnson, C.M.; Roden, E.E.; Beard, B.L. Coupled Fe(II)-Fe(III) electron and atom exchange as a mechanism for Fe isotope fractionation during dissimilatory iron oxide reduction. *Environ. Sci. Technol.* **2005**, *39*, 6698–6704.

(37) Ilina, S.M.; Poitrasson, F.; Lapitskiy, S.A.; Alekhin, Yu.V.; Viers, J.; Pokrovsky, O.S. Extreme iron isotope fractionation between colloids and particles of boreal and temperate organic-rich waters. *Geochim. Cosmochim. Acta* **2013**, *101*, 96-111.

(38) Kopácek, J.; Maresova, M.; Norton, S.A.; Porcal, P.; Vesely, J. Photochemical source of metals for sediments. *Environ. Sci. Technol.* **2006**, *40*, 4455–4459.

(39) Wu, L.L.; Beard, B.L.; Roden, E.E.; Johnson, C.M. Stable iron isotope fractionation between aqueous Fe(II) and hydrous ferric oxide. *Environ. Sci. Technol.* **2011**, *45* (5), 1847-1852.

(40) Skulan, J.L.; Beard, B.L.; Johnson, C.M. Kinetic and equilibrium Fe isotope fractionation between aqueous Fe(III) and hematite. *Geochim. Cosmochim. Acta* **2002**, *66*, 2995−3015.

(41) Frierdich, A.J.; Beard, B.L.; Reddy, T.R.; Scherer, M.M.; Johnson, C.M. Iron isotope fractionation between aqueous Fe(II) and goethite revisited: New insights based on a multi-direction approach to equilibrium and isotopic exchange rate modification. *Geochim. Cosmochim. Acta* **2014**, *139*, 383-398.

(42) Sun, R.Y.; Wang, B.L. Iron isotope fractionation during uptake of ferrous ion by phytoplankton. *Chem. Geol.* **2018**, *481*, 65-73.

(43) Vasyukova, E.V.; Pokrovsky, O.S.; Viers, J., Oliva, P., Dupré, B., Martin, F., Candadaup, F. Trace elements in organic- and iron-rich surficial fluids of the boreal zone: Assessing colloidal forms via dialysis and ultrafiltration. *Geochim. Cosmochim. Acta* **2010,** *74,* 449-468.

(44) González, A.G.; Pokrovsky, O.S.; Jiminez-Villacorta, F.; Shirokova, L.S.; Santana-Casiano, J.M.; González-Davila, M.; Emnova, E.E. Iron adsorption onto soil and aquatic bacteria: XAS structural study. *Chem. Geol.* **2014**, *372*, 32-45

(45) Viollier, E.; Inglett, P.W.; Hunter, K.; Roychoudhury, A.N.; Van Cappellen, P. The ferrozine method revisited: Fe(II)/Fe(III) determination in natural waters. *Appl. Geochem.* **2000**, *15* (6), 785-790.

(46) Mulholland, D.S.; Poitrasson, F.; Boaventura, G.R.; Allard, T.; Vieira, L.C.; Santos, R.V.; Mancini, L.; Seyler, P. Insights into iron sources and pathways in the Amazon River provided by isotopic and spectroscopic studies. *Geochim. Cosmochim. Acta* **2015,** *150,* 142-159.

(47) Ilina, S.M.; Drozdova, O.Y.; Lapitsky, S.A.; Alekhin, Yu.V.; Demin, V.V.; Zavgorodnaya, Yu.A.; Shirokova, L.S.; Viers, J.; Pokrovsky, O.S. Size fractionation and optical properties of dissolved organic matter in the continuum soil solution-bog-river and terminal lake of a boreal watershed. *Organic Geochem.* **2014,** *66,* 14–24.

(48) Gustafsson, J. Visual MINTEQ ver. 3.1. http://vminteq.lwr.kth.se, 2014, assessed 8.02.2019.

(49) Poitrasson F.; Freydier, R. Heavy iron isotope composition of granites determined by high resolution MC-ICP-MS. *Chem. Geol.* **2005,** *222,* 132–147.

(50) Mulholland, D.S.; Poitrasson, F.; Boaventura, G.R. Effect of different water storage procedures on the dissolved Fe concentration and isotopic composition of chemically contrasted waters from the Amazon River Basin. *Rapid Comm. Mass Spectr.* **2015,** *29,* 2102-2108.

(51) Kafantaris, F.C.A.; Borrok, D.M. Zinc isotope fractionation during surface adsorption and intracellular incorporation by bacteria. *Chem. Geol.* **2014,** *366*, 42–51.

(52) Croal, L.R.; Johnson, C.M.; Beard, B.L.; Newman, D.K. Iron isotope fractionation by Fe(II)-oxidizing photoautotrophic bacteria. *Geochim. Cosmochim. Acta* **2004**, *68*, 1227-1242.

(53) Bullen, T.D.; White, A.F.; Childs, C.W.; Vivit, D.V.; Schulz, M.S. Demonstration of significant abiotic iron isotope fractionation in nature. Geology **2001**, *29*, 699-702.

(54) Beard, B.L.; Handler, R.M.; Scherer, M.M.; Wu, L.; Czaja, A.D.; Heimann, A.; Johnson, C.M. Iron isotope fractionation between aqueous ferrous iron and goethite. *Earth Planet. Sci. Lett.* **2010**, *295* (1-2), 241-250.

(55) Dideriksen, K.; Baker, J.A.; Stipp, S.L.S. Equilibrium Fe isotope fractionation between inorganic aqueous Fe(III) and the siderophore complex, Fe(III)-desferrioxamine B. *Earth Planet. Sci. Lett.* **2008**, *269*, 280- 290.

(56) Morgan, J. L.; Wasylenki, L. E.; Nuester, J.; Anbar, A. D. Fe isotope fractionation during equilibration of Fe-organic complexes. *Environ. Sci. Technol.* **2010**, *44*, 6095−6101.

(57) Chupakova, A.A.; Chupakov, A.V.; Neverova, N.V.; Shirokova, L.S.; Pokrovsky, O.S. Photodegradation of river dissolved organic matter and trace metals in the largest European Arctic estuary. *Sci. Total Environ.* **2018**, *622–623*, 1343–1352.

(58) Barbeau, K.; Rue, E.; Bruland, K.; Butler A. Photochemical cycling of iron in the surface ocean mediated by microbial iron (III)-binding ligands. *Nature* **2001**, *413*, 409–413.

(59) Welch, S.A.; Beard, B.L.; Johnson, C.M.; Braterman, P.S. Kinetic and equilibrium Fe isotope fractionation between aqueous Fe(II) and Fe(III). *Geochim. Cosmochim. Acta* **2003**, 67(22), 4231–4250.

(60) Balci, N.; Bullen, T.D.; Witte-Lien, K.; Shanks, W.C.; Motelica, M.; Mandernack, K.W. Iron isotope fractionation during microbially stimulated Fe(II) oxidation and Fe(III) precipitation. *Geochim. Cosmochim. Acta* **2006,** *70,* 622–639.

(61) Teutsch, N.; Von Gunten, U.; Porcelli, D.; Cirpka, O.A.; Halliday, A.N. Adsorption as a cause for iron isotope fractionation in reduced groundwater. *Geochim. Cosmochim. Acta* **2005,** *69(17),* 4175–4185.

(62) Johnson, C.M.; Beard, B.L.; Roden, E.E.; Newman, D.K.; Nealson, K.H. Isotopic constraints on biogeochemical cycling of Fe. *Rev. Mineral. Geochem.* **2004,** 55, 359–408.

(63) Reddy, T.R.; Frierdich, A.J.;, Beard, B.L.; Johnson, C.M. The effect of pH on stable iron isotope exchange and fractionation between aqueous Fe(II) and goethite. *Chem. Geol.* **2015,** *397,* 118–127.

(64) Handler, R.M.; Beard, B.L.; Johnson, C.M.; Scherer, M.M. Atom exchange between aqueous Fe(II) and goethite: an Fe isotope tracer study. *Environ. Sci. Technol.* **2009,** *43(4),* 1102–1107.

(65) Chanda, P., Zhou, Z., Latta, D., Scherer, M., Beard, B., Johnson, C. Effect of organic C on stable Fe isotopic fractionation between aqueous Fe(II) and ferrihydrite. Goldschmidt Abstracts, **2018,** 365, https://goldschmidt.info/2018/abstracts/abstractView?id=2018003824.

(66) Anesio, A.M.; Granéli, W. Increased photoreactivity of DOC by acidification: Implication for the carbon cycle in humic lakes. *Limnol. Oceanogr*. **2003**, *48*, 735–744.

(67) Gao, H.; Zepp, R.G. Factors influencing photoreactions of dissolved organic matter in a coastal river of the southeastern United States. *Environ. Sci. Technol.* **1998,** *32*, 2940–2946.

(68) Wang, Y.; Xiang, W.; Yang, W.; Yan, S.; Bao, Z.; Liu, Y. Photo-stability of iron-phenolic complexes derived from peatland upon irradiation in waters under simulated sunlight. *Chem. Geol.* **2018**, *485*, 14-23.

(69) Helms, J.R.; Mao, J.; Schmidt-Rohr, K.; Abdulla, H.; Mopper, K. Photochemical flocculation of terrestrial dissolved organic matter and iron. *Geochim. Cosmochim. Acta* **2013**, *121*, 398–413.

(70) Catrouillet, C.; Davranche, M.; Dia, A.; Bouhnik-Le Coz, M.; Marsac, R.; Pourret, O.; Gruau, G. Geochemical modeling of Fe(II) binding to humic and fulvic acids. *Chemical Geol.* **2014**, *372*, 109-118.

(71) Dauphas, N.; John, S.G.; Rouxel, O. Iron isotope systematics. *Rev. Mineral. Geochem.* **2017**, *82*, 415-510.

(72) Drozdova, O.Yu.; Ilina, S.M.; Lapitsky, S.A. The transformation of dissolved organic matter in the soil water - bog - stream - terinal lake continuum of a boreal watershed (Northern Karelia), in: Pokrovsky, O.S., Shirokova, L.S., eds. *Dissolved Organic Matter (DOM): Properties, Applications and Behavior*, Nova Publishers, N.Y., 2017, pp. 115-133.

Table 1. Measured pH, DOC, Fe concentrations and isotopic ratios, relative to IRMM-14, during bio-and photo-degradation experiments. Note that the DOC in biodegradation experiments of stream water slightly increased due to cell lysis and exometabolite production. The standard error was calculated using the Student's t factor: SE = (t×SD)/√N , where N is the number of measurements.

Bio-degradation (1 g_{wet}/L of *Pseudomonas aureofaciens*)											
hrs	**Fen water ZPBL <0.22 µm**					**hrs**	**Stream water KAR-1 <0.22 µm**				
	pH	**DOC, mg L^{-1}**	**Fe, µg L^{-1}**	**Fe(II), µg L^{-1}**	**δ^{57}Fe ±2 SE, ‰**		**pH**	**DOC, mg L^{-1}**	**Fe, µg L^{-1}**	**Fe(II), µg L^{-1}**	**δ^{57}Fe ±2 SE, ‰**
0	4.9	37.4	2470±45	645±20	1.06±0.05	0	6.6	12.4	180±10	30±20	2.87±0.07
1	5.2	37.0	1690±20	620±20	0.86±0.07	1	6.4	13.6	115±7	< LOQ*	2.54±0.06
8	5.4	35.8	1520±20	290±10	0.85±0.12	8	6.4	13.0	82±10	< LOQ*	2.68±0.16
22	5.7	34.8	1365±15	no data	0.88±0.07	22	6.7	14.0	63±3	< LOQ*	3.21±0.15
30	5.8	26.6	1290±5	145±5	0.99±0.10	50	7.0	14.1	56±2	< LOQ*	3.26±0.13
50	5.8	23.3	1197±5	120±10	1.03±0.05	100	7.2	15.2	50±2	< LOQ*	no data
100	6.1	25.2	1054±5	84±5	1.04±0.04						
Sunlight exposure											
hrs	**Fen water ZPBL <0.22 µm**					**hrs**	**Stream water KAR-1 <0.22 µm**				
0	5.4	38.7	4310±100	840±50	0.25±0.07	0	7.2	11.9	208±20	50±20	1.59±0.05
100	5.1	20.3	1840±400	770±170	-0.8±0.38	110	6.8	10.4	193±25	60±25	1.75±0.2
200	5.3	18.7	915±30	450±10	-2.63±0.03	250	6.7	8.2	175±25	15±5	2.1±0.12
hrs	**Fen water ZPBL <10 kDa**					**hrs**	**Stream water KAR-1 <10 kDa**				
0	5.3	26.5	1125±50	620±20	0.19±0.02	0	6.8	10.2	35±5	20±10	2.93±0.06
100	5.2	18.7	1000±50	510±20	-1.98±0.13	110	6.9	10.0	49±10	30±20	1.95±0.06
200	5.3	17.9	945±50	470±30	-2.49±0.15	250	6.8	8.1	14±2	< LOQ*	1.89±0.07
hrs	**Fen water ZPBL <1 kDa**					* Limit of quantification					
0	5.6	10.6	200±20	70±10	-0.18±0.03						
100	5.3	11.5	560±30	300±100	-2.34±0.11						
200	5.4	16.8	620±30	340±100	-2.43±0.12						

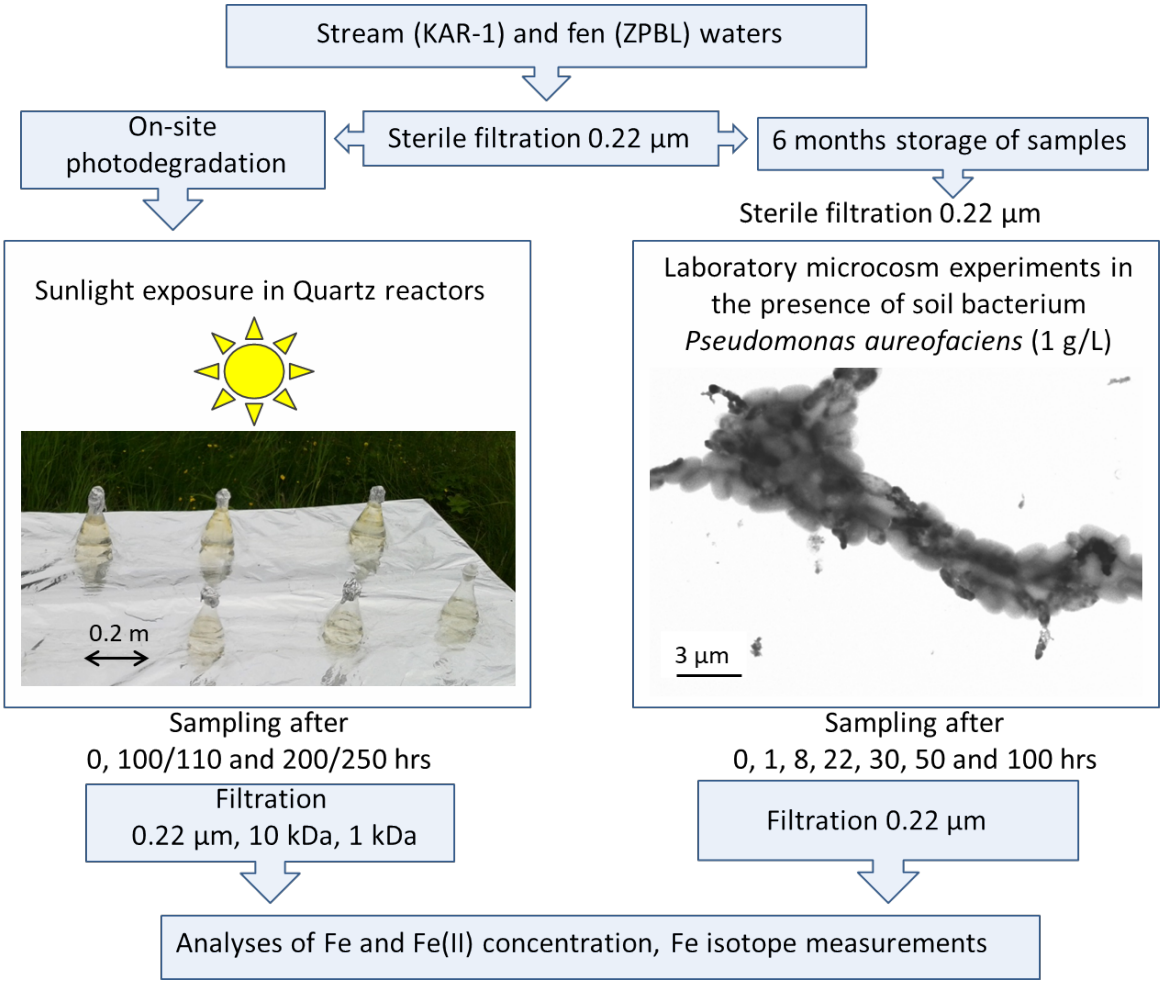

716

717 **Fig. 1.** Conceptual scheme of experiments (run in duplicates): a photo of quartz reactors exposed to
718 sunlight and a Transmission Electron Microscopy (TEM) image of bacterial cells with
719 precipitated Fe hydroxides. The photodegradation experiments were performed on-site,
720 immediately after water sampling and sterile filtration. The biodegradation experiments
721 required sterile laboratory environments and were run after 6 months of water storage. The
722 biodegradation experiments included only < 0.22 µm filtration after sampling. In
723 photodegradation experiments, the stream water was processed for the < 0.22 µm and the <
724 10 kDa filtration and the fen water was filtered through 0.22 µm, 10 kDa and 1 kDa.

725

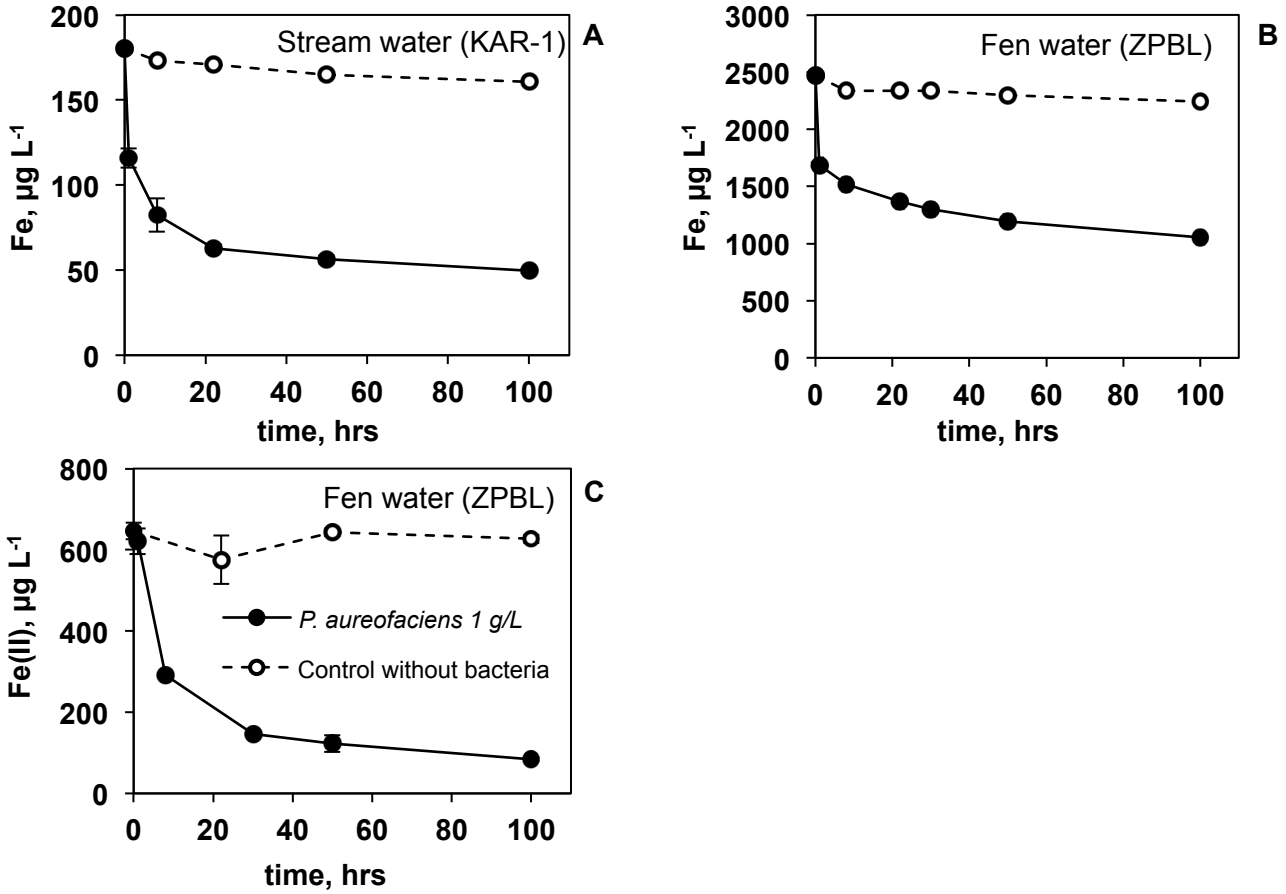

726 **Fig. 2.** Evolution of total dissolved Fe concentration during biodegradation experiments of stream
727 (**A**) and fen (**B**) water. **(C):** Fe(II) concentration evolution in the fen water during
728 biodegradation. The error bars of biotic experiments represent 1 SD of duplicates. In most
729 cases, they are smaller than the symbol size. Bacterial experiments are shown by solid
730 circles and bacteria-free control is represented by open circles for all three panels as
731 indicated in (C). A 10 to 12 % decrease of Fe concentration in the bacteria-free control
732 experiment may be due to precipitation of small amount of Fe(III) hydroxide.

733

734

735

736

737

738

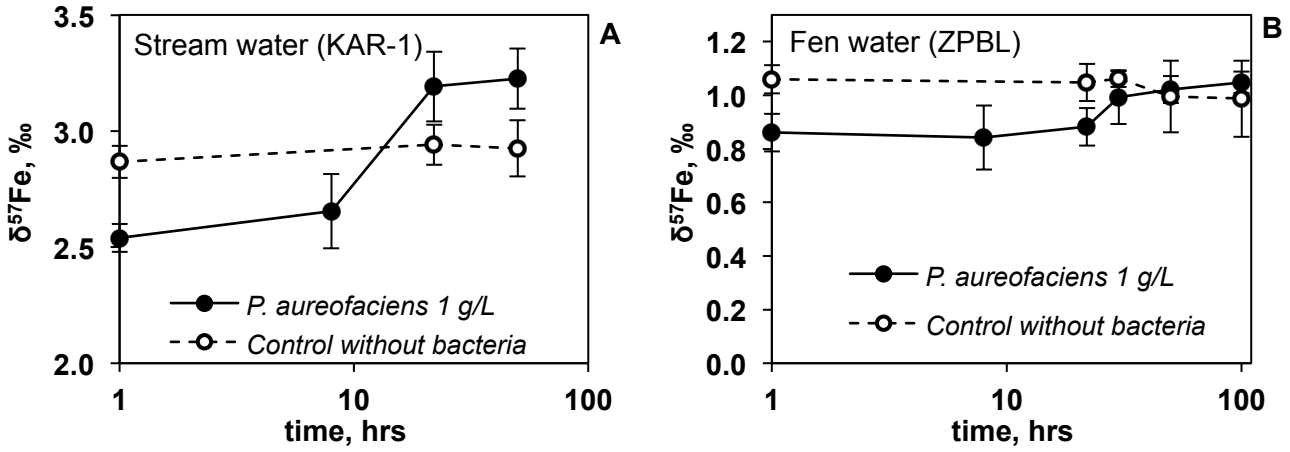

739

740 **Fig. 3.** Evolution of isotopic ratios δ^{57}Fe during biodegradation experiments of stream (A) and fen
741 (B) water. Note log scale for time axis..

742

743

744

745

746

747

748

749

750

751

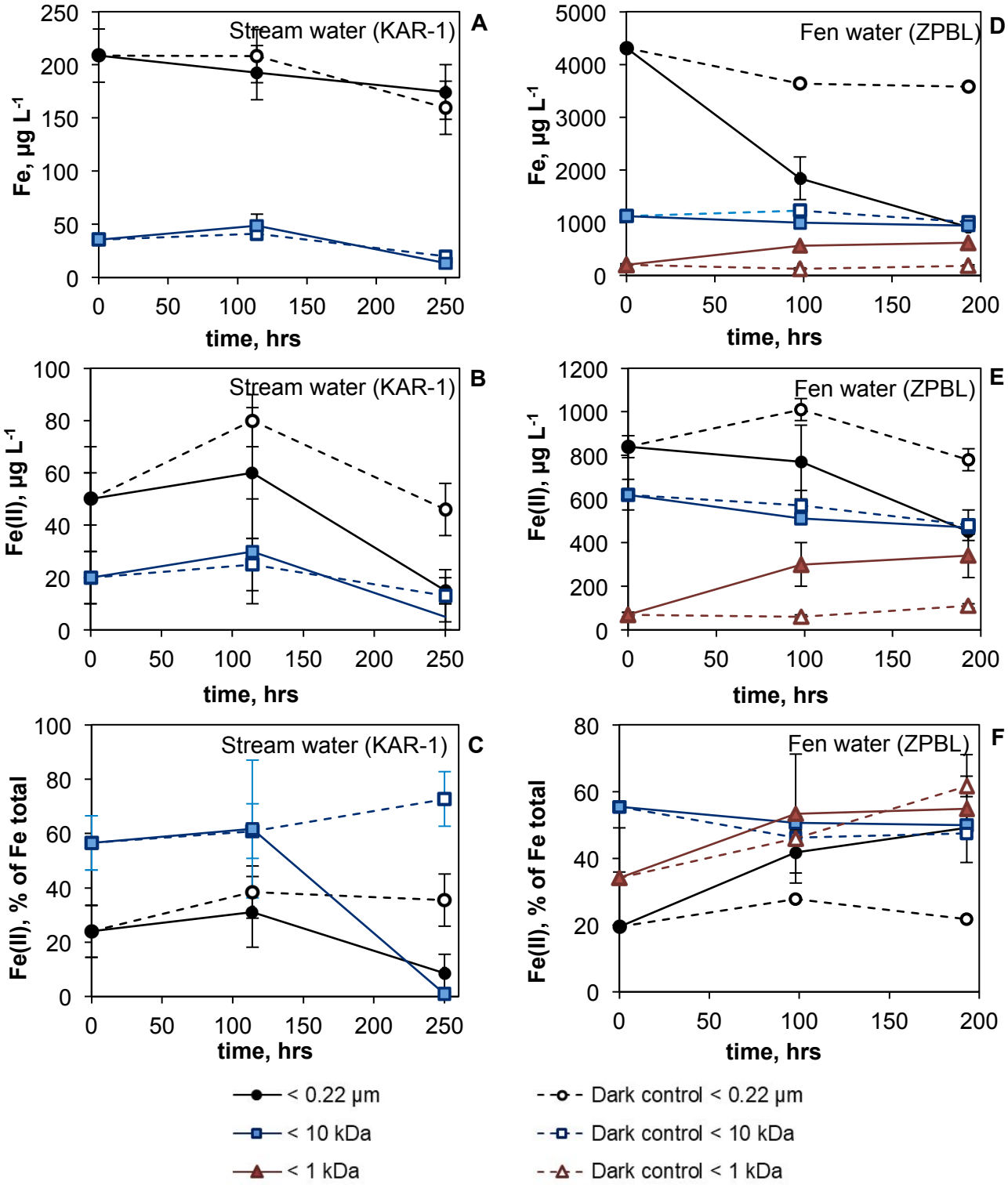

752 **Fig. 4.** Evolution of Fe_{tot} and Fe(II) concentration during photodegradation experiments of
753 stream (**A, B, C**) and fen (**D, E and F**) water in quartz reactors. Note a drop in Fe_{tot} and Fe(II)
754 concentration of the < 0.22 µm dark control at 200 and 250 h not observed in previously stored
755 samples in biodegradation experiments (Fig. 2), which may be due to partial precipitation fo Fe(III)
756 hydroxide in freshly sampled natural water upon storage.
757
758

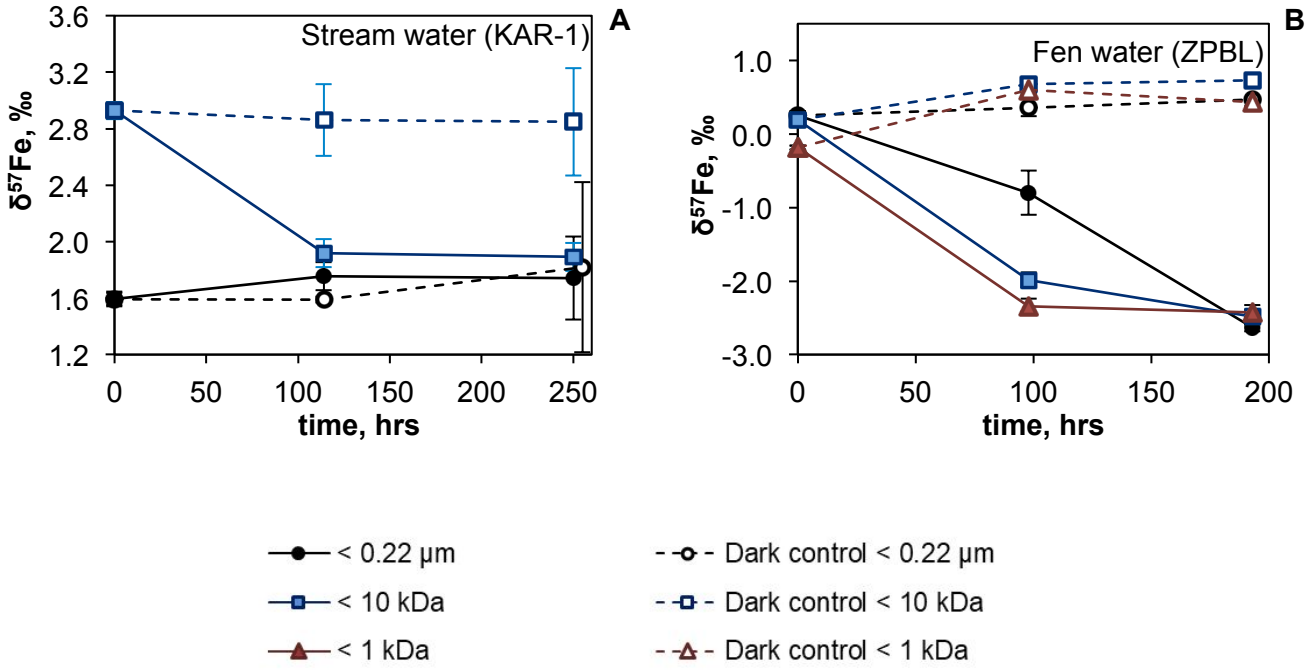

759

760 **Fig 5.** Evolution of isotopic ratios δ^{57}Fe during photodegradation experiments of stream (A) and fen
761 (B) water. There is a clear decrease in δ^{57}Fe value in all fractions of photodegraded samples
762 of fen water, but this decrease is only pronounced for the < 10 kDa fraction of stream water.
763 Note that a weak increase in δ^{57}Fe for the <0.22 µm dark control in KAR-1 is within the
764 uncertainty of replicates. An increase in δ^{57}Fe for the < 1 kDa and < 10 kDa dark control of
765 fen waters is due to Fe loss of these unstable, freshly sampled waters.

766

767

768

769

770

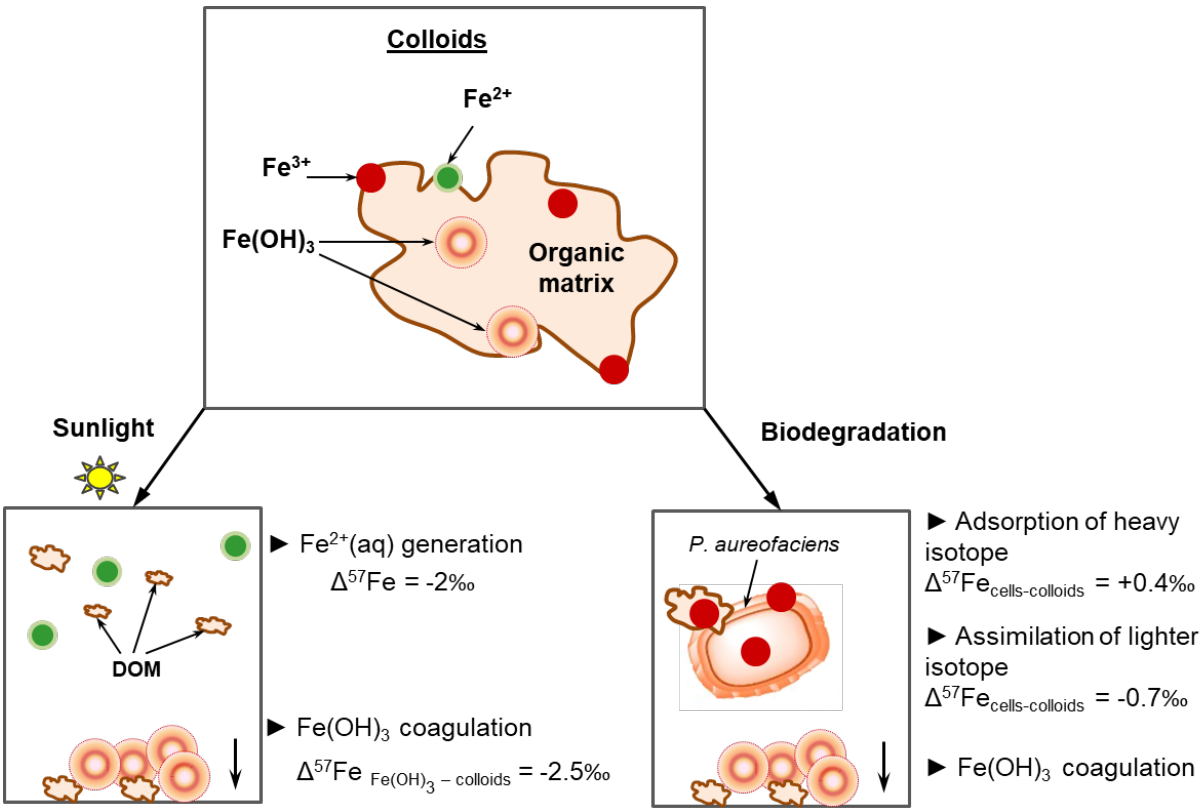

Fig. 6. Cartoon of Fe isotope fractionation under sunlight-induced transformation (left) and biodegradation (right) of organic and organo-ferric colloids (1 kDa - 0.22 µm). Live heterotrophic *P. aureofaciens* bacteria adsorb heavier and assimilate lighter Fe isotopes. Sunlight irradiation generates isotopically light Fe(II) in low molecular weight (< 1 kDa) fraction and produces heavy isotope enrichment in particulate fraction relative to total dissolved (< 0.22 µm) form. After bio- or photo-degradation of organic matter which constitutes organo-ferric colloids, the liberation of Fe(III) ions and precipitation of Fe(III) hydroxide occur. This removes heavier isotopes from solution into the solid phase. Altogether, bio-and photodegradation of organo-ferric colloids can produce very Fe) large, from -2 to +3‰ isotopic variations (δ^{57}Fe) in boreal humic waters.

796
797 **SUPPORTING INFORMATION:**

798 **Measured pH, DOC, Fe concentrations and isotopic ratios in control reactors used in bio-and**
799 **photo-degradation experiments; results of vMinteq calculation of Fe(II) and Fe(III) speciation**
800 **in experimental solutions**

801

SUPPORTING INFORMATION:

Measured pH, DOC, Fe concentrations and isotopic ratios in control reactors used in bio-and photo-degradation experiments; results of vMinteq calculation of Fe(II) and Fe(III) speciation in experimental solutions

Table S1. Measured pH, DOC, Fe concentrations and isotopic ratios, relative to IRMM-14, in control reactors used in bio-and photo-degradation experiments. Note that abiotic < 0.22 µm controls of biodegradation experiments were more stable in terms of both [Fe] and δ^{57}Fe than the dark controls of photodegradation experiments. Freshly sampled natural water used for photodegradation experiments could be subjected to certain transformation, re-equilibration and even coagulation of Fe and DOC. In contrast, aged filtered water was used in biodegradation experiments and it produced more stable pattern of concentration and isotope signature in control reactors.

Bio-degradation control reactors											
hrs	**Fen water (ZPBL) < 0.22 µm**					**hrs**	**Stream water (KAR-1) < 0.22 µm**				
	pH	**DOC, mg L^{-1}**	**Fe, µg L^{-1}**	**Fe(II), µg L^{-1}**	**δ^{57}Fe ±2 SE, ‰**		**pH**	**DOC, mg L^{-1}**	**Fe, µg L^{-1}**	**Fe(II), µg L^{-1}**	**δ^{57}Fe ±2 SE, ‰**
0	4.9	37.4	2470±45	645±20	1.06±0.05	0	6.6	12.4	180±10	30±20	2.87±0.07
8	4.9	35.2	2339±30	no data	no data	8	6.6	12.2	173±10	20±10	no data
22	5.0	37.7	2335±30	576±60	1.05±0.07	22	6.6	12.7	171±10	no data	2.94±0.09
30	5.1	37.0	2335±30	no data	1.06±0.03	50	6.8	12.5	164±10	30±20	2.93±0.12
50	5.1	36.9	2295±30	643±10	1±0.13	100	6.9	12.1	160±10	<LOQ*	no data
100	5.1	36.5	2242±30	627±10	0.99±0.14						
Sunlight exposure control reactors											
hrs	**Fen water (ZPBL) < 0.22 µm**					**hrs**	**Stream water (KAR-1) < 0.22 µm**				
0	5.4	38.7	4310±100	840±50	0.25±0.07	0	7.2	11.9	208±20	50±20	1.59±0.05
100	5.4	35.3	3630±50	1010±70	0.36±0.14	110	7.0	11.5	210±30	80±10	1.59±0.02
200	5.3	37.0	3580±50	780±70	0.47±0.03	250	6.8	11.8	160±30	46±10	1.82±0.60
hrs	**Fen water (ZPBL) < 10 kDa**					**hrs**	**Stream water (KAR-1) < 10 kDa**				
0	5.3	26.5	1125±50	620±20	0.19±0.02	0	6.8	10.2	35±5	20±10	2.93±0.06
100	5.4	25.2	1230±50	570±70	0.68±0.01	110	7.1	8.3	40±5	25±10	2.86±0.25
200	5.4	22.2	1010±50	480±70	0.73±0.04	250	6.8	8.4	20±5	15±10	2.85±0.38
hrs	**Fen water (ZPBL) < 1 kDa**					* Limit of quantification					
0	5.6	10.6	200±20	70±10	-0.18±0.03						
100	5.8	5.3	122±20	60±10	0.60±0.07						
200	5.7	9.0	182±20	110±10	0.43±0.07						

Table S2. Calculated speciation using vMINTEQ of Fe(II) and Fe(III) in < 0.22 µm fraction of stream and fen water at the beginning (0 h) and after 100 h of biodegradation experiments. FA stands for Fulvic Acid.

Iron	Species name	Fen water (ZPBL) < 0.22 µm		Stream water (KAR-1) < 0.22 µm	
		% of total Fe(II) or Fe(III) concentration			
		0 h	100 h	0 h	100 h
Fe(II)	Free ions	1.73	0	0	0
	Weakly (electrostatically) bound with FA	30.33	0.01	0	0
	Complex with FA's carboxylic groups	67.94	99.98	99.99	100.00
Fe(III)	Complex with FA's carboxylic groups	26.82	6.83	0.28	0.07
	Complex with FA's phenolic groups	73.18	93.17	99.72	99.93

Table S3. Speciation of Fe(II) and Fe(III) in < 0.22 µm fraction of stream and in < 0.22 µm and < 1 kDa fractions of fen water at the beginning (0 h) and after 200-250 h of sunlight exposure. FA stands for Fulvic Acid.

Iron	Species name	Fen water ZPBL < 0.22 µm		Fen water ZPBL < 1 kDa		Stream water KAR < 0.22 µm	
		% of total Fe(II) or Fe(III) concentration					
		0 h	200 h	0 h	200 h	0 h	250 h
Fe(II)	Free ions	0.26	3.40	0.01	3.40	0	0
	Weakly (electrostatically) bound with FA	56.53	12.33	18.46	12.33	0	0
	Complex with FA's carboxylic groups	43.21	84.26	81.53	84.26	99.99	100.00
Fe(III)	Complex with FA's carboxylic groups	6.60	2.20	6.60	2.20	0.11	0.32
	Complex with FA's phenolic groups	93.40	97.81	93.40	97.81	99.89	99.68

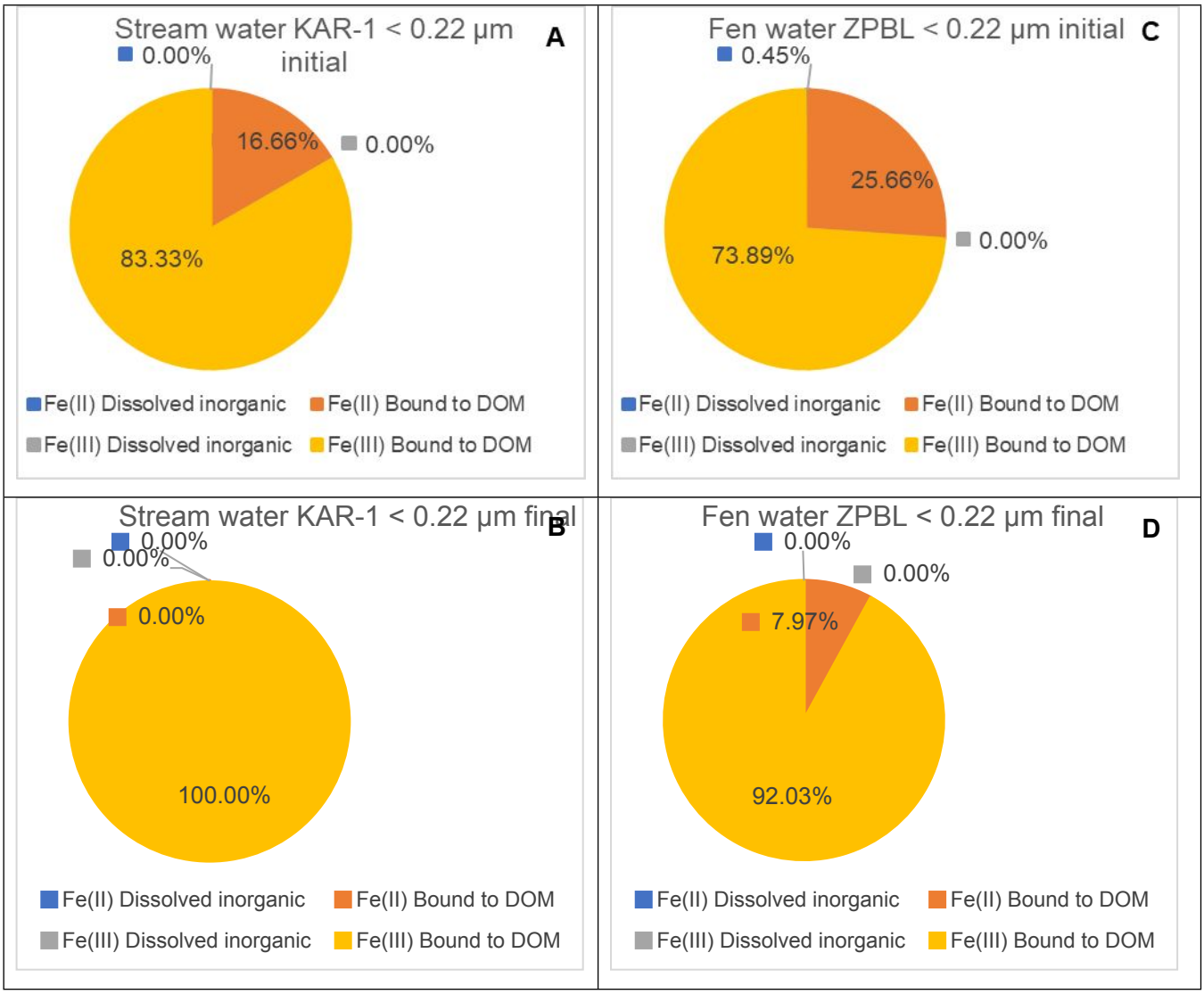

Fig. S1. Results of vMINTEQ speciation calculation for initial (0 h) and final (100 h) solutions during biodegradation experiments with stream (**A, B**) and fen (**C, D**) water.

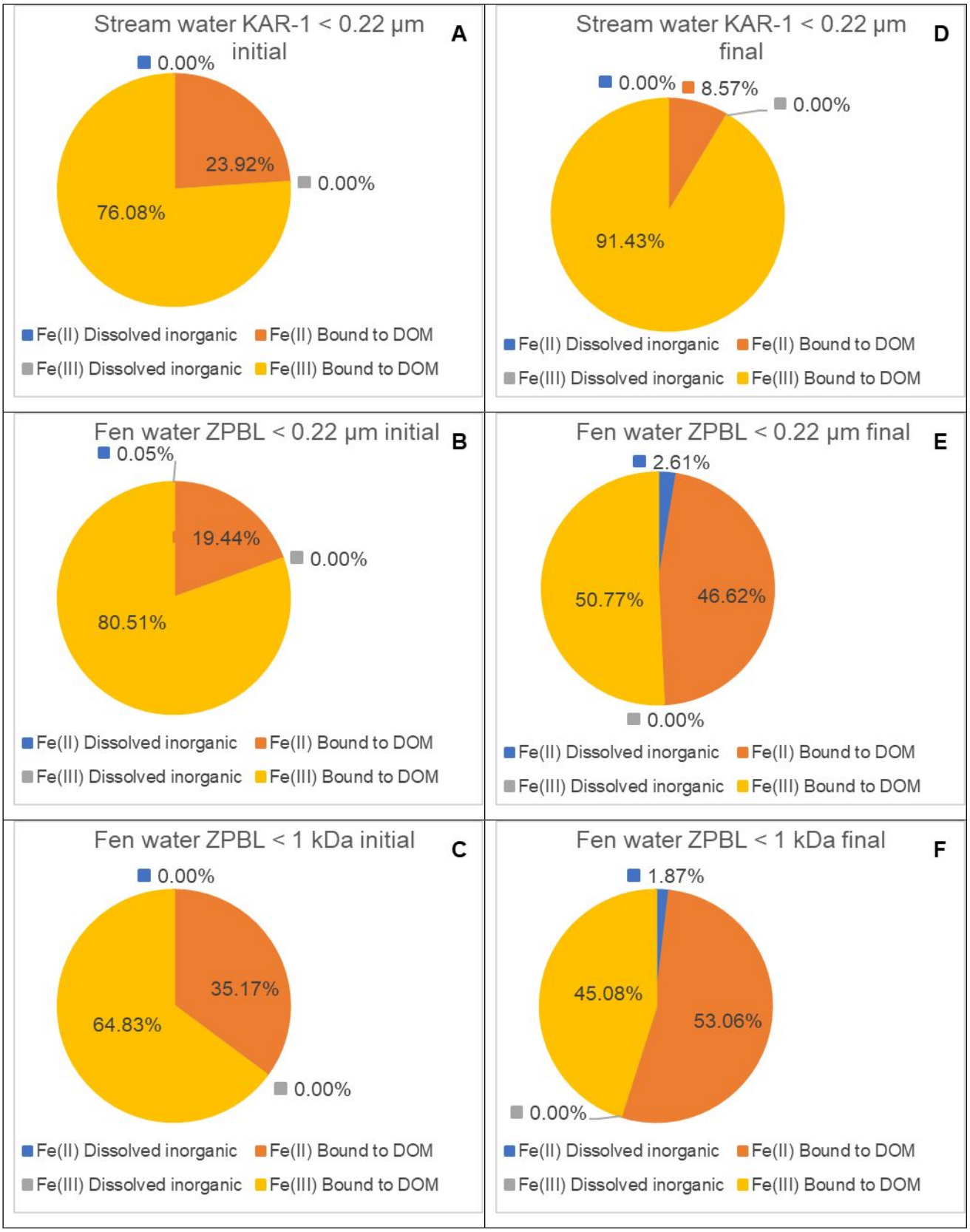

Fig. S2. Results of vMINTEQ speciation calculation for initial (0 h) and final (200-250 h) solutions during photodegradation experiments with stream (**A, D**) and fen (**B, C, E, F**) waters.